GuarddoG Project

DRAFT / WORK IN PROGRESS

Author : Ammar Qammaz
Supervisor : Georgios Papaioannou

Athens , January 2012

Introduction and motivation
Goal
Overview

Introduction and motivation

A few opening remarks

Humans increased their physical power during the industrial revolution using machines. They were able to create giant dams , factories , cars , airplanes and skyscrapers to make their everyday life easier . Technology has continued to improve exponentially and in the current age , labeled by some as the age of informatics or the internet , mental capabilities where multiplied. Merging the following two revolutions we can finally partly replace ourselves from dull and repetitive tasks of day to day life that will gradually stop to trouble the human kind leading to a more pleasant life. The GuarddoG project is about making machines that can see and act as a futuristic private guard .

The process of creating an autonomous robot that can perceive its environment and react and interact with it took nature millions of years. From the first bacteria to multi cell organisms , the wolf then the dog and the human , enormous evolutionary differences created beings of immense complexity and perfection. For someone to build something that took such a great amount of time in even a quarter of a lifetime is over-ambitious. An extra observation that is thought provoking is that while humans in complex decision making such as chess playing or tactic games with a limited set of rules have been surpassed by computers. In contrast in simple things for humans such as perceiving space , time , and "natural logic" every human has an innate superiority a result of the millions years of natural selection with these characteristics as a basis.

That being said GuarddoG does not attempt to create a dog (with everything a dog implies) , because this is practically impossible. Its goal is replacing a specific function of a dog as a guardian. I am very optimistic that with time robots will eventually be improved enough to be able to perform a multitude of tasks approaching something that will surely be different than a real dog , better at some things , and worse at some others.

Even though the future will offer even more tools , even now thanks to the marvelous technology and work of all the scientists , mathematicians , physicists , chemists , engineers and computer scientists (we are literally standing on the shoulders of giants)   I was able to construct something very close to my original target , spending a fraction of the money and time that would be required before 15 or even 10 years.

A better way for someone to visualize the small subset of functionality that is attempted by computer vision algorithms and in this case GuarddoG , is to compare it to the holy grail of cognition and intelligence , the human brain. Though computers for many years have managed to surpass human experts on tasks like playing chess , remembering sequences of numbers , performing arithmetic calculations on large data sets and recently even guessing questions to answers (IBM Watson on the Jeopardy TV Show) , things that everyone can do without even thinking about , like walking , identifying 3D objects and faces , and coordinating his head , eye and body movement are currently unachievable by machines at least to the extent of human performance .

This is a good indicator of the level of optimization that has taken place through the millions of years of evolution , because there is no doubt that if playing chess was a trait that leaded to natural selection the human brain would be totally different and have a much greater affinity towards these kind of activities. On the other hand , if breathing , beating the heart or walking and identifying objects wasn't crucial for the survival of the human species , to master these kind of activities could may well be as difficult and time consuming to be achieved as mastering chess .
*

Project Goal

The goal of the "Guard Dog" Project

The goal of the Guard Dog Project is to build a robotics platform that can act as a guard , traverse a known path and fend off intruders. In case of a security breach it would signal the alarm and begin to follow the perpetrator and after a set distance would resume its previous path.

Robotics and computer vision are not a new domain of computer science and electrical engineering. It was especially shocking for me to see video footage of experiments in the AI Lab of Stanford (for example Les earnest and Lou paul and the Rancho Arm) circa 1971 that perform object detection , complex decision making and that actually use more or less the same algorithms as current robotics projects do. The major difference is not so much about the methods used , but the exponential improvement on computer hardware , popularly coined as Moore`s Law.

We are living in times where many high-end mobile phones actually have more complex processors than the satellites of the first mission to the moon and that experiments such as those that required equipment that cost millions of dollars in 1971 and could only be done in universities or government research centers can be reproduced with consumer electronics readily available everywhere. Unfortunately the consistent computation of the world around a robot is still a very difficult and expensive task with a generic CPU and no specialized hardware , but yet it seems almost feasible when you achieve even something that can work 10 times slower than a human.

Of course an additional goal of the project is to perform guard duties using only cheap building blocks but not passive sensors as modern security systems do. Instead building a semi-intelligent agent that can do this job the way humans would do it. It is an exploration of the possibilities and limits of current technologies along with software that can leverage the capabilities of computer hardware in an efficient way, to achieve an almost working result.

It is also interesting to note that the same computer vision libraries can , with adjustments , be fitted for tasks like driving cars in city streets to helping blind people find their way or any task that involves using optical information of ones surroundings to achieve a related goal.
The main difference would be the risk/cost and risk/performance ratio since a computer driving a car at full speed can do much worse damage when compared to a small robot bumping on a wall.

*

Overview

An outline of this text to help the reader

The ease with which humans sense the world makes the problem of computer vision seem "easy" to solve. In fact the way we see is so natural and persistent that even scientists in the field made biased over-optimistic predictions about it. The fact is that despite the exponential growth in computational speed , and although there is a very big market that could certainly use vision algorithms to automate tasks , there is still no defacto algorithm that can compare to what human vision performs. Moreover from simple reflexes as maintaining focus and coordinating ones gaze , reading text , to tracking your position in an unknown city , vision seems to be "AI-Complete" , since understanding and combining what is seen is an altogether different task than the small building blocks which are presented here.

A robot that can see and interact with the world , is basically a Turing machine on wheels. Therefore the whole model presented here is an adaptation of different mathematical concepts and a fusion of them together. The strip of tape in this Turing machine is constantly filled with symbols of light intensity as the light gets reflected and activates the camera sensor elements. When the control algorithm decides that the robot has to move it writes it to the according tape elements and the motors move , producing a new view of the world.
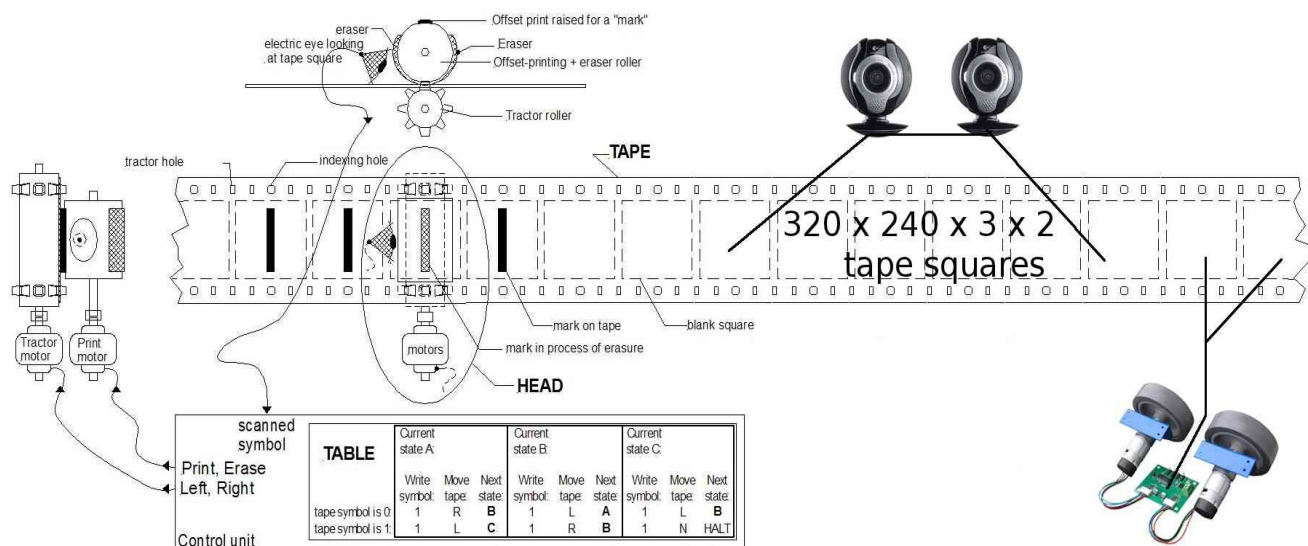
A fanciful mechanical Turing machine's TAPE and HEAD. The TABLE instructions might be on another "read only" tape, or perhaps on punch-cards. Usually a "finite state machine" is the model for the TABLE.

The first thing to take into consideration beginning to approach this problem , is how the physical world is being represented by the cameras. They are , after all , the means with which the GuarddoG/RoboVision algorithm collection , a "meta"physical entity can take a peek into reality. The data acquired must then be filtered to remove deformations and distortions that may corrupt the whole process. These steps are described in the Camera Model , Camera Calibration and Image Rectification parts of this document. Once two corresponding images of the projection of the world on the camera sensors are aquired , they are examined for optical cues that reveal the details of the world in three dimensions and also the robot's position. This is also discussed extensively , and the Disparity Mapping algorithm used by GuarddoG is a new implementation. When all these steps are finished , the next one is tracking the position of the robot (LK Optical Flow , RANSAC Homography) and the combination of the successive 3d Views together (SLAM , Obstacle Detection).
The final piece of the algorithm is a knowledge base that will set its goals and keep the state of the world , and steer the robot towards achieving them. For GuarddoG , its goal is the traversal of a standard path , and raising the alarm if a breach is found.
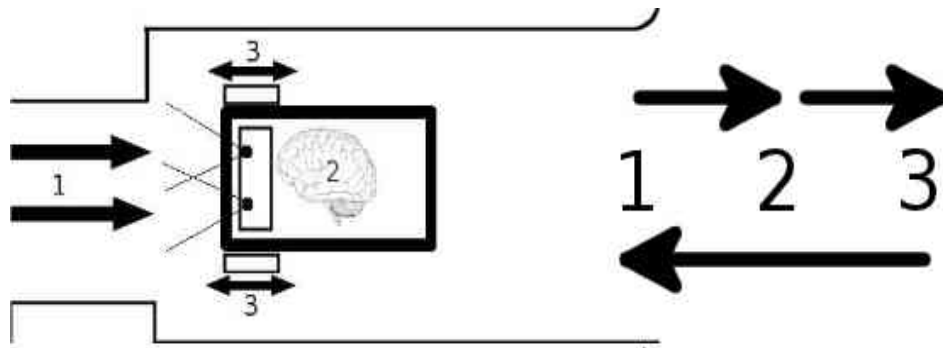

Illustration 1: The chicken and egg problem nature of an autonomous robot , that with its action changes its perception of the world , and with the changing perception of the world it changes its action..!

When beginning to make a system that sees , one can make many choices about the way with which to gather input. As nature teaches us , and by bringing to mind various insects and animals that have been optimized through a process of millions of years to see one might use anything from ultrasonic sounds , to millions small eyes of insects up to human stereoscopy. With the world represented through the camera being so chaotic , and as this project does not deal with a fixed environment in which to be operated , while also having economic restrictions applied the best choice was a human like stereoscopic camera input. It is true that commercial RGB+depth cameras such as Microsoft Kinect can bypass a very big portion of the computational complexity of this project , but they still have their own drawbacks. The stereoscopic setup wasn't chosen by accident by nature , and the nature of a robot that uses stereoscopic vision makes it closer to the human experience as a mode of viewing the world.

Illustration 2: What computers see

Trying to approach the computational limit of a dense stereoscopic method for two frames sized 320x240 pixels in order for a full search from an image patch sized 40x40 pixels on the left eye to all the possible matching patches along the epipolar line on the right eye , we have to make 320 x 320 x 240 / 40 = 24576000 /40 = 614400 operations in the worst case each time we get a depth map. In order to achieve a "human like" response time from the vision system this has to be done at a rate of 25 frames per second , or with a delay of 40 milliseconds per scan..

The number of operations per second increases exponentially as the image size becomes larger

SIZE	IMAGE RESOLUTION	OPERATIONS	OPERATIONS PER ms
QVGA	320 x 320 x 240 / 40	24,576,000	614,400 operations / ms
VGA	640 x 640 x 480 / 40	196,608,000	4,915,200 operations / ms
XGA	1024 x 1024 x 768 / 40	805,306,368	20,132,659 operations / ms
...	Other Configurations	...	...
WUXGA	1920 x 1920 x 1024 / 40	3,774,873,600	94,371,840 operations / ms
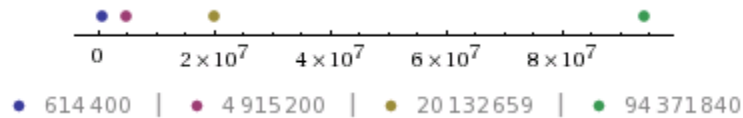
This exponential increase , of course , impacts all the algorithms used on the project , and for every operation there are numerous sub operations implied so the total maximum number of operations ends up being many times larger than the numbers on this table. All the algorithms on the other hand do a better job than this worst case scenario , and specifically the disparity mapping algorithm of GuarddoG , which is one of its novel aspects and is briefly presented in this text . To reduce the number of operations by design , and as an early measure to compensate for the cheap hardware that is used by the onboard computer the resolution of images used by default is QVGA (320x240 pixels) .

Manufacturing a physical stereo rig for the experiments which is perfectly aligned has a crucial effect on the calculations. Not only it increases computational efficiency and reduces errors but it also removes mathematical ambiguity about instances of the world that can be interpreted in many ways.. The relative position of the GuarddoG cameras is supposed to be constant and the two cameras always have a coplanar alignment with a fixed distance between the optical centers. The cameras are also never allowed to change their focus (nor could change it as they do not have an automatic focus control).
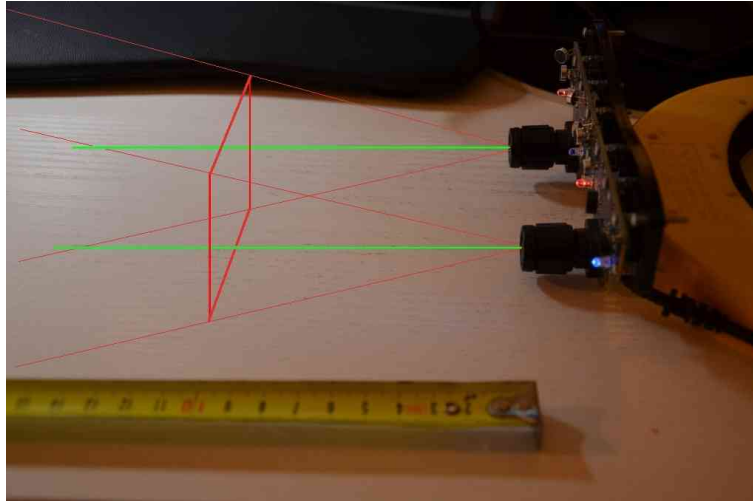

Illustration 3: The fixed parallel camera rig , that GuarddoG uses

<chk>

To avoid re calculations and use of the CPU for reasons avoidable by better designed algorithms or a smarter implementation , the whole vision library uses a pipelined architecture , so that the same image will not have to pass a processing stage twice once it enters and according to the needs of the Robot Hypervisor the different stages try to be combined , or operations stay pending for the next frame.

The pipeline itself , a term that is frequently mentioned in this document , is an abstract term meaning the whole library collection and the final program which when executed receives input from the cameras , channels it and processes it and then using the motor system steers the whole platform to achieve the set goal .

The purpose of this document is to describe and analyze this pipeline and it is organized in five parts , each of which is dedicated to a certain aspect of it. The first stage is to analyze the mathematical background of the algorithms , why they were chosen and why they should in theory work discussing performance issues from a complexity viewpoint .

The second part focuses on hardware and technical details , along with performance statistics for different hardware setups

The third one explains the various tactics followed writing the software and how everything fits together on the resulting software stack.

Part four discusses about the system in practice , its performance and limitations on actual deployment , and the fifth and the last chapter for future plans for an even better implementation .
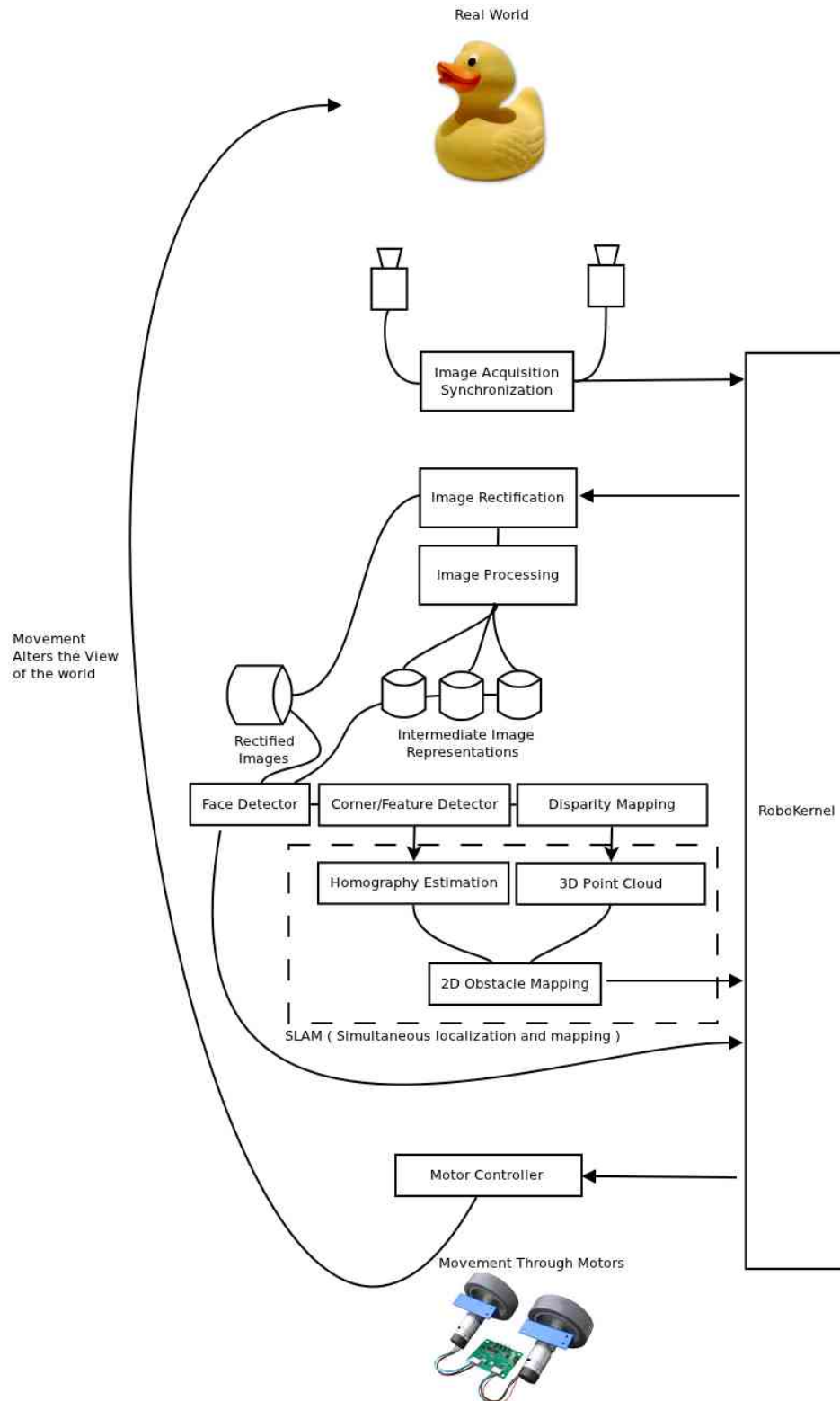
Illustration 4: A schematic of the pipeline of data as they go through the system. This image is the connection diagram for all the methods presented here

*</chk>

Mathematical Framework

1.1.1 Camera Pinhole Model

A pinhole camera is a light capturing device without lens and a very small aperture. Regardless of the imaging sensor , the shutter system , or the integrated circuit on camera , it is fundamental to understand the physical model and how light gets projected on the sensor , in order to start to reverse engineer the physical process that creates the data we acquire.

The smaller the hole of the camera , the sharper the image gets , but as the hole size decreases , so does the total number of photons that pass through it, resulting in a dimmed image for short exposures.

The pinhole camera model applies to most consumer grade web cameras , but it can not be used without some additional processing overhead due to manufacturing inefficiencies that distort the projection on the camera sensor. These are discussed in the calibration and re sectioning parts of this document , that repair the distorted image making it fit to the ideal pinhole camera model described here.

*

Illustration 5: The pinhole camera model , illustration from Wikipedia , public domain

-

The point O is where the camera aperture is located , and the start of the axes. The three axes of the coordinate system are referred to as X1, X2, X3. Axis X3 is pointing in the viewing direction of the camera and is referred to as the optical axis, principal axis, or principal ray. The 3D plane which intersects with axes X1 and X2 is the front side of the camera, or principal plane.

An image plane where the 3D world is projected through the aperture of the camera. The image plane is parallel to axes X1 and X2 and is located at distance f from the origin O in the negative direction of the X3 axis. A practical implementation of a pinhole camera implies that the image plane is located such that it intersects the X3 axis at coordinate -f where f > 0. f is also referred to as the focal length of the pinhole camera.

A point R at the intersection of the optical axis and the image plane. This point is referred to as the principal point or image center.

A point P somewhere in the world at coordinate (x1,x2,x3) relative to the axes X1,X2,X3.

The projection line of point P into the camera. This is the green line which passes through point P and the point O.

The projection of point P onto the image plane, denoted Q. This point is given by the intersection of the projection line (green) and the image plane. In any practical situation we can assume that x3 > 0 which means that the intersection point is well defined.

There is also a 2D coordinate system in the image plane, with origin at R and with axes Y1 and Y2 which are parallel to X1 and X2, respectively. The coordinates of point Q relative to this coordinate system is (y1,y2).

*

Illustration 6: The pinhole camera model , viewed from the side (from the X2 axis) , illustration from Wikipedia , public domain

The geometry of the pinhole camera viewed from the side , and on two dimensions. The calculations performed are based on similar triangles that are created with the point O as their intersection.

The mathematical equations that condense are the following :

$$\frac{-y_1}{f} = \frac{x_1}{x_3} \vee y_1 = -f\frac{x_1}{x3}$$

$$\frac{-y_2}{f} = \frac{x_2}{x_3} \vee y_2 = -f\frac{x_2}{x3}$$

$$(y_1 y_2) = \frac{-f}{x_3}(x_1 x_2)$$
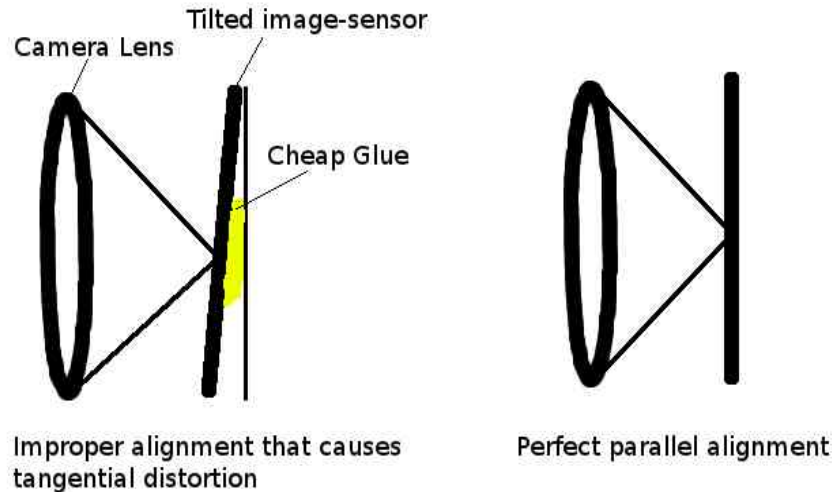
*

Mathematical Framework

1.1.2 Camera Calibration

Having explained the underlying geometry behind the ideal pinhole camera model we need to adapt it to real cameras and their physical limits. In mathematics, it is possible to define a lens set that will introduce no distortions in the image captured. In practice, however, and due to manufacturing process inefficiencies two types of distortion occur . Radial distortion , caused by the shape of lens not being parabolic , and tangential distortion due to the assembly process of the camera in the factory.

Radial distortion causes a characteristic bending of straight lines as they get closer to the edges of the image and on systems that are heavily based on those images it can have a very detrimental effect on calculations that gets worse as the errors gradually accumulate in time. While disparity mapping algorithms can partly withstand this kind of distortion due to using a relatively large neighborhood of pixels that overall remains the same , point tracking and optical flow algorithms that estimate and track the camera position are very vulnerable to this kind of distortion.The reason this happens is because the relative positions of pixels change as they move to the edges and give wrong constraints for the system of equations to be solved later on.

| Barrel distortion | Pincushion distortion |

Tangential Distortion on the other hand is a matter of misplacing the imaging sensor relatively to the lens (not a fully parallel placement) and therefore receiving a slightly skewed image.

Camera Lens   Tilted image-sensor

Cheap Glue

Improper alignment that causes tangential distortion

Perfect parallel alignment

Figuring out the way with witch a camera distorts the projection of the world on to its image sensor is called camera calibration. There are numerous methods and considerations to be taken into account to achieve calibration , even methods that gradually "auto calibrate" the raw input images without special patterns and objects or prior training of the algorithm. [citations needed] . GuarddoG uses a much more common approach , acquiring the intrinsic camera parameters (explained in the next chapter) using a fixed chessboard pattern that on the calibration stage is expected to be moved across the visible image so that enough snapshots of data can be acquired that may lead to a precise calculation . The method used by OpenCV is [citation needed] and the pattern is for GuarddoG is a 10x7 chessboard. After OpenCV finds the calibration parameters , they are stored in a file and used by GuarddoG's pipelining as the first processing step after an image is acquired.

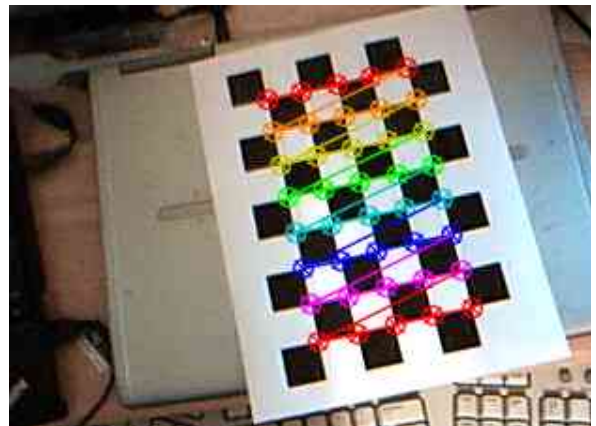*Illustration 7: OpenCV Chessboard 10x7 calibration pattern*

Illustration 8: Typical Detection Image Generated by OpenCV

The OpenCV implementation receives the corners between the chessboard blocks as inputs , which are extracted using a corner detector.   First, it computes the initial intrinsic parameters and sets the distortion coefficients to zero. Afterwards using the Levenberg-Marquardt optimization algorithm [citation needed] the reprojection error is minimized until a stable parameter set is found.

A thing that is worth to be mentioned is that the cameras used by GuarddoG are graded by the manufacturer to have a less than 5% distortion and the algorithms work sufficiently well even when input is uncalibrated.

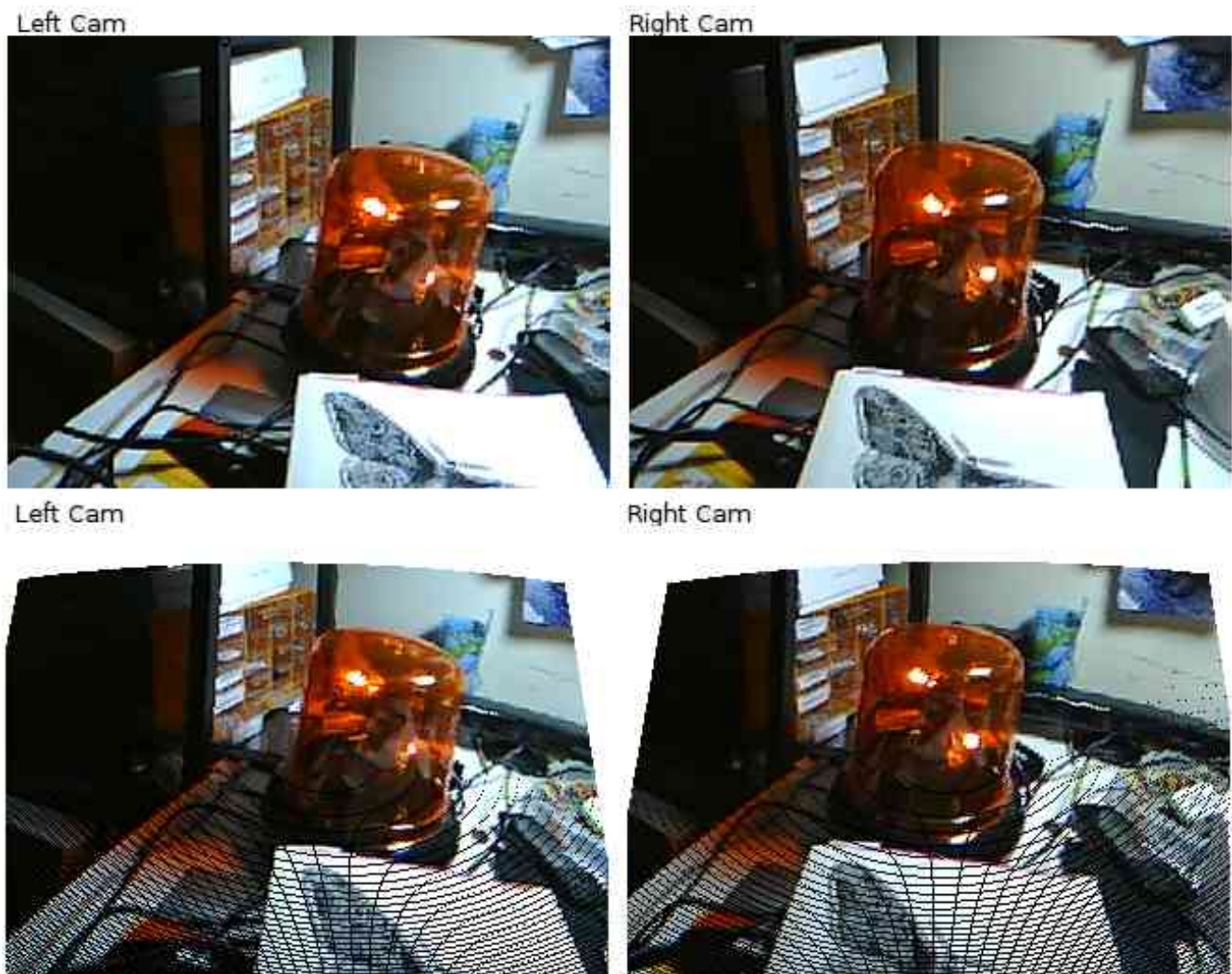The method was conceived by Zhang [citation needed] and Sturm [citation needed]

Illustration 9: Raw images received from the cameras and their calibrated equivalent (the distortion parameters are exaggerated to better show the way calibration alters the input images)

*

Mathematical Framework

1.1.3 Image Rectification

Each camera has intrinsic and extrinsic parameters. Intrinsic parameters model the camera as a device and they are constituted by the skew coefficient (γ) that is a coefficient that is usually zero , the principle point or image center (Cx , Cy) and Fx , Fy which is the focal point multiplied by a number that scales from pixels to distance (and is defined by the size of a pixel in the image sensor) .

Extrinsic parameters give information about the position of the camera in the world , and are basically a translation and a rotation matrix , usually combined in a 3x4 matrix.

The extended equations from the pinhole model for a perfect undistorted lens with with intrinsic and extrinsic parameters are modeled by the following equations

$$
s \begin{pmatrix} u \\ v \\ 1 \end{pmatrix} = \begin{pmatrix} f_x & \gamma & c_x \\ 0 & f_y & c_y \\ 0 & 0 & 1 \end{pmatrix} \begin{pmatrix} r_{11} & r_{12} & r_{13} & t_1 \\ r_{21} & r_{22} & r_{23} & t_1 \\ r_{31} & r_{32} & r_{33} & t_1 \end{pmatrix} \begin{pmatrix} X \\ Y \\ Z \\ 1 \end{pmatrix}
$$

$$
\begin{pmatrix} x \\ y \\ z \end{pmatrix} = R \begin{pmatrix} X \\ Y \\ Z \end{pmatrix} + t
$$

$$
x' = x/z
$$
$$
y' = y/z
$$

$$
u = f_x x' + c_x
$$
$$
v = f_y y' + c_y
$$

x' and y' are used as an intermediate step to better show the
added computations when performing resectioning in the page that follows

Radial and tangential distortion correction gets included to the model using k1 , k2 , k3 coefficients for radial distortion and p1 , p2 for tangential. They basically works by warping the image with a center of cx,cy and the higher the distance from the center the more it is pushed away.

$$s\begin{pmatrix} u \\ v \\ 1 \end{pmatrix} = \begin{pmatrix} f_x & 0 & c_x \\ 0 & f_y & c_y \\ 0 & 0 & 1 \end{pmatrix} \begin{pmatrix} r_{11} & r_{12} & r_{13} & t_1 \\ r_{21} & r_{22} & r_{23} & t_1 \\ r_{31} & r_{32} & r_{33} & t_1 \end{pmatrix} \begin{pmatrix} X \\ Y \\ Z \\ 1 \end{pmatrix}$$

$$\begin{pmatrix} x \\ y \\ z \end{pmatrix} = R \begin{pmatrix} X \\ Y \\ Z \end{pmatrix} + t$$

$$x' = x/z$$
$$y' = y/z$$

$$r^2 = x'^2 + y'^2$$

$$x'' = x'(1 + k_1 r^2 + k_2 r^4 + k_3 r^6) + 2 p_1 x' y' + p_2(r^2 + 2x'^2)$$
$$y'' = y'(1 + k_1 r^2 + k_2 r^4 + k_3 r^6) + p_1(r^2 + 2y'^2) + 2p_2 x' y'$$

$$u = f_x x'' + c_x$$
$$v = f_y y'' + c_y$$

Executing these calculations gives us the rectified position of a point captured by the camera.</chk>

Since re sectioning the image must be done for every frame received from the usb cameras (which serve images @ 120 Hz) and since most camera chips don't offer a hardware interface for passing the distortion parameters to the local integrated circuit so it can perform this kind of image processing with out involving the main processor , a fast technique must be applied to avoid calculating all these displacements on every new frame.

Since the camera doesn't change its focus settings , the distortion parameters are always the same. We can use this knowledge to our advantage generating a precalculation frame that has pointers to the calibrated positions as its elements after acquiring the distortion parameters.
That way , the expensive task of computing the formulas mentioned above happens only once and the least possible overhead is added to the pipeline process (around 500 microseconds per frame on the main development computer , hardware details are on the second part of this text).

This tactic is followed both by the OpenCV implementation , as well as the GuarddoG RoboVision stack.

*

Mathematical Framework

1.2.0 Image Processing

   Digital cameras are devices that capture the light that the universe reflects on their sensor. The general problem most vision algorithms try to solve is guessing what kind of a world reflects the light in that way. The algorithms presented here are building blocks that gradually transform the raw RGB input into more computationally meaningful representations . <chk>
  Convolution is a mathematical operation applied to sets of values that "redistributes" them according to coefficients from a second set of values. The result is a new combined set that has similarities with both previous sets. Convolution is originally defined in mathematical functional analysis and takes a slightly different form in image processing where it is typically performed on a 2D array of brightness values.   The carrier of the weights is called a convolution matrix and its elements act as coefficients changing the neighboring elements of each pixel. The larger the convolution matrix size , the smoother the redistribution , but due to the computational cost the most common sizes for kernels are 3x3 or 5x5 with usually the middle pixel used as a point of reference or an anchor point. </chk>
   The values transformed by the convolution matrix are the red , green and blue light intensities of the pixels retrieved from the image sensor. In the following example we assume a 3x3 kernel and a monochrome image sensor that captured 9x6 pixels. The kernel is passed left to right and up to down until all of the elements are changed. GuarddoG uses Blur , First and Second Derivative Convolution kernels that follow with example images.

1	1	1
1	**1**	1
1	1	1

3X3 Convolution Kernel
Divisor 9

As the anchor of the kernel passes from each element of the image array the value (marked blue) gets replaced by the addition of the neighboring elements multiplied with the corresponding kernel coefficients.

$$H(x,y)=\sum_{i=0}^{Mi-1}\sum_{j=0}^{Mj-1} I(x+i-a_i, y+j-a_j)G(i,j)$$

The anchor element on the light intensities array will become
(1x90+1x80 +1x70+1x90+1*80+1*70+ 1x90 + 1x80 + 1x70) / 9 which is 80

9 x 6 Original Light Intensities Captured

90	80	70	90	80	70	90	80	70
90	80	70	90	80	70	90	80	70
90	80	70	90	80	70	90	80	70
90	80	70	90	80	70	90	80	70
90	80	70	90	80	70	90	80	70
90	80	70	90	80	70	90	80	70

 An important thing to be noted Is that values on the edges of the array (marked orange) can not be correctly calculated as not all neighboring elements exist , common solutions for this is zero padding , using a different divisor to compensate for the missing elements or skipping the elements that can not be calculated correctlly .

BLUR FILTER **(Gaussian Approximation)**			
	1	2	1
	2	**4**	2
	1	2	1
		Divisor 16	

FIRST-ORDER DERIVATIVE **(Horizontal Sobel)**			
	1	2	1
	0	**0**	0
	-1	-2	-1
		Divisor 1	

FIRST-ORDER DERIVATIVE **(Vertical Sobel)**			
	-1	0	1
	-2	**0**	2
	-1	0	1
		Divisor 1	

SECOND-ORDER DERIVATIVE			
	-1	0	1
	0	**0**	0
	1	0	-1
		Divisor 3	

<chk>

As someone can easily observe by thinking a little about the convolution process , it is a waste of resources to perform multiplications with the null elements of a convolution matrix, and as an example for the second-order derivative that has 5 null elements a little more than half the original number of multiplications can be skipped. An additional optimization that can be performed is combining two convolution matrices in to one to reduce memory access related latencies from two subsequent passes on the image.

Horizontal				Vertical				Combined on		
1	2	1		-1	0	1		p1	p2	p3
0	**0**	0		-2	**0**	2		p4	**p5**	p6
-1	-2	-1		-1	0	1		p7	p8	p9
Divisor 1				Divisor 1						

The values p1 … p9 are the pixel values on the image array in which the convolution takes place..
In order to completely avoid multiplications (at least on the matrix part) we add and subtract the values and so for the pixel 2 (p2) since the coefficient is 2 we do p2 + p2 .

horizontal_sum = p1 + p2 + p2 + p3 - p7 - p8 - p8 - p9
vertical_sum = p1 + p4 + p4 + p7 - p3 - p6 - p6 - p9

final_sum = square_root((horizontal_sum * horizontal_sum) + (vertical_sum*vertical_sum))

The final speed up is replacing the square root operation with a log base 2 approximation using shift operations based on the IEEE 754 floating point arithmetic standards and the algorithm described below.

```
inline float square_root (const float x)
{
  union
  {
    int i;
    float x;
  } u;
  u.x = x;
  u.i = (1<<29) + (u.i >> 1) - (1<<22);
  return u.x;
}
```

Of course using an SIMD (Single instruction, multiple data) instruction set capable CPU with properly aligned data and loop unrolling can speed up the operations even more but even without these steps , the code form on this level is simple enough for gcc to do a good job optimizing it automatically.

Blur filters even out the colors on an input image using the median color value of the surrounding area . Blurring is a common operation by vision software mainly used due to the fact that image sensors retrieve pixels that suffer from noise , these noise spikes are reduced therefore leading to more stable edge and corner detection.

The First-order derivative operator acts as a differentiation operator , resulting in an output that only responds to "change" of colors and ignores similar colored areas. Thus it is very useful as it reduces the image to its more unique parts , its edges .

The second-order derivative operator also acts as a differentiation operator , resulting in an output that only responds to "change" of "change" of colors (second order) and ignores similar colored areas while also having a better reaction to sudden spikes on the color frequency. Its output also reveals the image edges but is much more stable than the first-order operator.

Palette reduction reduces the total number of possible tones that one pixel can take from 16581375 on an 24bit color depth (255 * 255 * 255) to an other given number. Reducing the total possible colors causes similarly colored pixels to fall into the same color bin. This can be leveraged to make the datasets more resistant to noise. Conversion from a full color palette to a monochrome image , is a very common operation on computer vision algorithms.

Thresholding can be used as a filter extension to apply a high (or low) pass bound on an incoming signal and discard pixels that do not match the criteria. This is generally done after edge detection operations to reduce false output caused by noise.

The RGB Movement operation is a direct absolute subtraction of each of the pixels (on each of the color channels). This is passed through a low threshold and results on an output image with a large value where there is a large color difference (movement) and 0 value when the pixel remains unaltered This "delta" version of two images is useful in many occasions. First in determining if the stream of images is static , (so we can skip redundant calculations and improve the performance and power consumption of the CPU) , it is important when the robot is not moving and views a supposedly still environment as a really fast alarm function and it helps with disparity mapping , since unoc

Histograms are produced by counting the total instances of the different colors on an area of an input. They can provide a good general idea about an image , such as its brightness, color distribution and are used in guarddog as a fast discarding mechanism for regions of the image when performing disparity mapping .

The miscellaneous image processing operations used by GuarddoG are mentioned in the table that follows
</chk>

NAME	OPERATIONS	DESCRIPTION
Gaussian Blur	9 * Height*Width	Blurring input image to reduce noise
Sobel edge det.	2 * 9 * Height*Width	Edge Detection
Second-order de.	4 * Height*Width	Edge Detection
Palette Reduce	Height*Width	Group color frequencies together to reduce them
Threshold Image	Height*Width	Discard information that may be subject to noise
RGB Movement	3*Height*Width	Subtract row RGB values from two consecutive images
Histogram	Height*Width	Calculate number of pixels that have the same color

*

Mathematical Framework
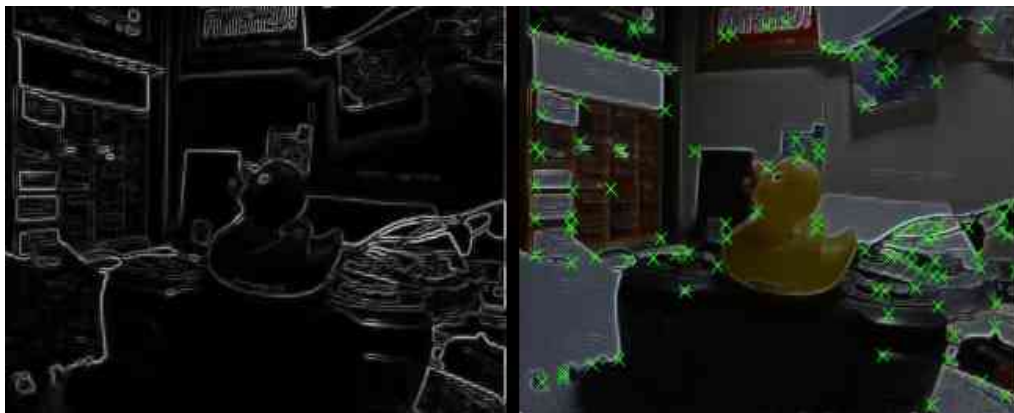
1.2.1 Corner and Feature Detection

Illustration 10: Left : An incoming image after passing through First-order Derivative Edge detection , Right : The corners detected , highlighted with green X marks

After performing the various image processing steps mentioned above , to start moving away from the image as a raw array of color frequencies and into a better representation , we must focus on specific points on it that stand out and have unique characteristics . These points are called features or salient points and can be picked using a multitude of methods. The features used by GuarddoG are corners and offer a good performance and quality trade-off. They are both relatively inexpensive computationally to extract and also exhibit persistence between frames produced from small movement of the camera , in normal indoor lighting conditions.
<chk>
Some feature detectors such as SURF [citation needed] pick points that not necessarily lie in a corner , but nevertheless have a large eigen value and are scale and rotation resistant. The feature detector used by GuarddoG is built with high performance in mind (and thus lower average quality of feature points) and is called FAST [citation needed]. It classifies a point as a possible corner by casting a bresenham circle of radius 3 around it. Thus from the 16 points casted if the intensities o f at least 12 contiguous pixels are all above or all below the intensity of the central point by some threshold it returns a match. </chk>

Illustration 11: An instance of the algorithm detecting a feature (corner) by sampling the 16 points of the circle casted around the point 7,4 using the FAST algorithm. The detector finds two similar colored points and succeeds in detecting the corner.

<chk>A second feature detector that is used as a lower performance higher quality alternative and performs adequately is the OpenCV cvGoodFeaturesToTrack method by Shi and Tomasi [citation needed]. which utilizes a second-derivative filtered image. It then calls cvCornerMinEigenVal and cvCornerEigenValsAndVecs to pick the minimum eigen values under a threshold and again provides a list of good features on a reasonable computational cost. The inner workings of the algorithm are based on texturedness criteria that are reflected by the eigenvalues. Two small eigen values mean a roughly constant intensity profile within a window, a large and a small eigen value , a unidirectional texture pattern and two large eigen values patterns that can be tracked reliably such as corners. All these are extensively discussed in the original paper.

$$M = \begin{pmatrix} \sum (dI/dx)^2 & \sum (dI/dx * dI/dy) \\ \sum (dI/dx * dI/dy) & \sum (dI/dy)^2 \end{pmatrix}$$

The minimal eigenvalue is then picked since:
$$x_1, y_1 \text{ corresponds with } \lambda_1$$
$$x_2, y_2 \text{ corresponds with } \lambda_2$$

and compared to a threshold

A typical image retrieved from the camera consists of a finite number of pixels. The corners returned by the algorithms mentioned above are integers but in reality it is very improbable for a corner to lie exactly on the center of a pixel. This inaccuracy is enough to effectively derail the pose tracking algorithm that takes the corners as its only input and has a tendency to accumulate errors and thus we need more detail about where the corners truly lie. A detected pixel with coordinates (123,69) given as a result from the algorithms above may be fine tuned to a real number such as (123.349 , 69.512) for example.
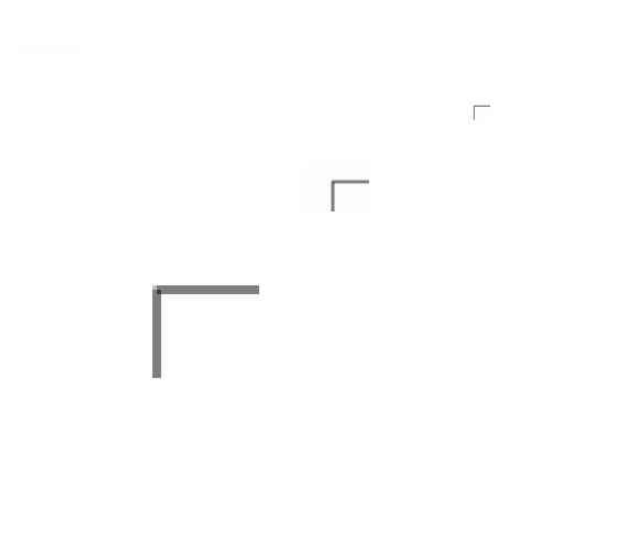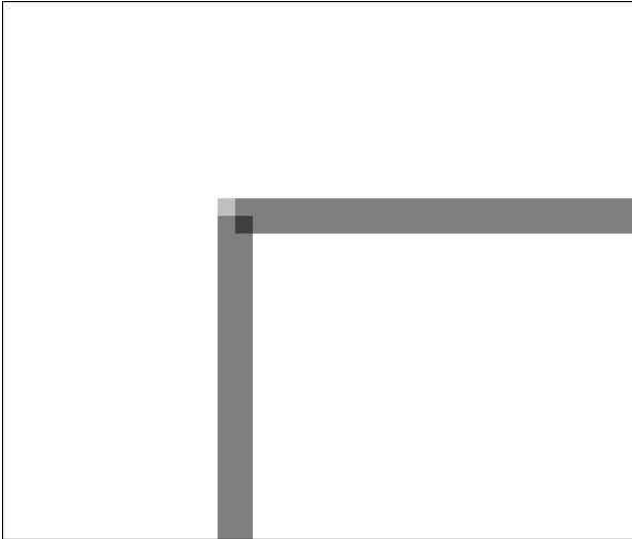
Illustration 12: Left : In which pixel exactly does the corner lie ? Right : As the same corner image is viewed from increased distance (or in a increased resolution) the inaccuracy gets smaller compared to the total area covered

To start approximating the new corner we have to build up a system of equations that when solved will give us a sub pixel approximation. The OpenCV method for this work is called cvFindCornerSubPix and it uses simple vector algebra to achieve it. It is based on the fact that the dot product of orthogonal vectors is zero and if one of the two vectors does not exist (is zero) it is again zero. This forms several equations that are all equal to zero which when solved provide a better set of coordinates for the corner.

Illustration 13: A hypothetical point p and the two vectors that lead to it from point original corner point q

Illustration 14: A hypothetical point p on the same line with q

$$\langle \nabla I(p), q-p \rangle = 0$$

The dot product of the Gradient of pixel p with q – p is in both cases zero

With a system of enough p points the point q is re positioned with better precision but the process can be repeated with as many iterations needed until an accepted accuracy is achieved. For example to achieve a tenth of a pixel accuracy , the process must be repeated until two subsequent q approximations differ less than 0.10 pixels .
*</chk>

Mathematical Framework

1.2.2 Template Matching and Integral Images

MAJOR TODOS HERE :'(: The image processing pipeline receives raw input from the cameras and produces images that are

After image processing is finished producing "versions" of the data that reveal different aspects of the input images , the next technique performed by guarddog is called Template Matching.
There are numerous criteria that can be used to compare two image parts and decide if they match.

GuarddoG uses a combination of pyramid segmentation , feature and template based matching across different templates to achieve high performance without sacrificing result quality. To this end the use of integral images speeds up and greatly improves the algorithm (performance-wise) .

The most simple and computationally efficient method for comparing two blocks of pixels is named SAD (Sum of Absolute Differences) and is basically the following equation.

$$SAD = \sum_{x=0}^{width} \sum_{y=0}^{height} |(image1[x][y] - image2[x][y])|$$

 This operation can be hardware accelerated on MMX and SSE2 instruction capable CPUs and thus is very lite weight. Although there are other metrics to find out if two image blocks match (and how similar they are) such as MSE (Mean Squared Error) , SATD (Sum of absolute transformed differences) , Normalized Cross Correlation (NCC) and other even more complex methods.

To make up for quality loss , while keeping the increased performance that SAD offers guarddog compares different "versions" of the patches that resulted mainly from convolution operations on the original data. That way the computational cost is moved from the block matching operation that can be performed millions of times (especially in large images) and does not take a guaranteed time to converting the image itself which has a fixed sized.

The different SAD results are then combined into a single value according to weights to compensate for the different range of values in each of the sub images. In order to further skip unneeded calculations a local histogram is used as a threshold that can completely avoid calculations if the 2 image blocks bear no resemblance at all (i.e. one is completely white and the other completely black)

*

Illustration 15: The things taken into account when comparing patches

Before going into more detail about the template matching function , another useful representation for massive calculations on images is called integral images , or summed area tables.

$$I(x',y')=\sum_{x=0}^{x'}\sum_{y=0}^{y'}(image[x][y])$$

Once the table that every x,y has as an element the I(x,y) is created . We can skip a huge number of adding operations for an arbitrary area of the image (limited only by the maximum value of an integer on the machine). Any block addition operation is thus reduced to 4 operations.

$$\sum_{x=x1}^{x2}\sum_{y=y1}^{y2}image[x][y]=I(x1,y1)+I(x2,y2)-I(x2,y1)-I(x1,y2)$$

The resulting operation is not SAD because the subtraction does not produce an absolute difference on each pixel , the resulting operation is a plain Sum of Differences which is an even worse metric than SAD but it has such a big performance impact , that when used in conjunction with the sub images mentioned before it can make dense disparity mapping feasible , and when used in small enough areas provides good overall results.

Instead of :
|image1[x1][y1] – image2[x1][y1]| + |image1[x2][y1] – image2[x2][y1]| + … + |image1[xN][yN] – image2[xN][yN]|
we have

image1[x1][y1] + image1[x2][y1] + … + image1[xN][yN] - (image2[x1][y1] + image2[x2][y1] + … + image2[xN][yN])
which is the same with

image1[x1][y1] – image2[x1][y1] + image1[x2][y1] – image2[x2][y1] + … + image1[xN][yN] – image2[xN][yN]
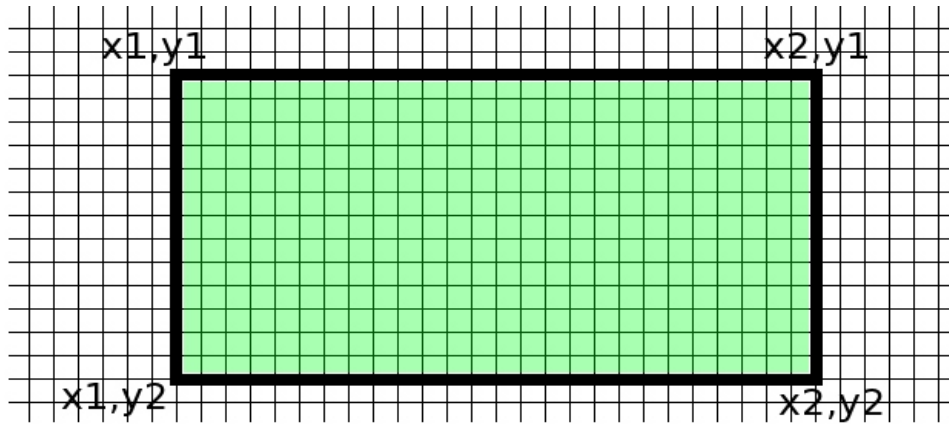
*

Illustration 16: Typically , we find the sum of the green area by adding all the pixels in it performing (x2-x1)*(y2-y1) operations

Illustration 17: We can find the sum of the green area by performing 4 operations , I(x1,y1)+I(x2,y2)-I(x1,y2)-I(x2,y1) provided we have first calculated the integral array I

Illustration 18: A SAD metric returns total mismatch of these two blocks. An addition of differences metric (not absolute) such as the integral imaging technique described before returns a total match of the two image blocks

*

Mathematical Framework

1.2.2 HAAR Wavelet Face Detection

Haar-like features are digital image features used in object recognition. Their similarity with Haar wavelets is what gave them their name and they were used in the first real-time face detector. GuarddoG uses the OpenCV implementation of a haar cascade detector with an appropriate training file , while the implementation is largely based on the Viola Jones Face detection algorithm (Robust Real-time Object Detection) [citation needed].

There are many approaches to face detection and as a refinement recogniton , including eigen faces (M. Turk and A. Pentland (1991). "Face recognition using eigenfaces") , image pyramids (Neural Network-Based Face Detection, 1998), and mixed methods (W. Kienzle, G. Bakir, M. Franz and B. Scholkopf: Face Detection - Efficient and Rank Deficient. In: Advances in Neural Information Processing Systems 17, pg. 673-680, 2005.) , each of which have their own pros and cons .

The reason for choosing a Haar feature based face detection is that it is again accelerated by integral images and thus it can fit in nicely in the pipeline of the vision processor algorithm while performing incredibly well for upright faces that are the only kinds of faces that a small indoor robot should normally respond to.

A Haar Wavelet is a small region that consists of two areas , one black (low value) and one white (high value) . As a pattern it can have a lot of iterations , and the ones displayed bellow are the most common ones. To decide if a feature is present , a simple sum operation is performed on each of the two areas and then the intensity difference is calculated between the white and black areas.

Illustration 19: Common Haar Wavelets
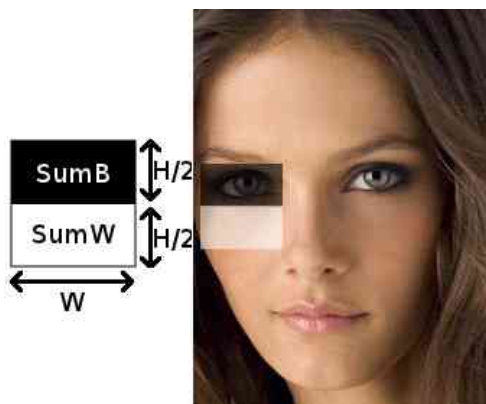
SumB = The Sum of color intensities in black area
SumW = The Sum of color intensities in white area

FeatureValue = SumW – SumB

If (FeatureValue > Threshold) { FeatureValue=1 }
                       else   { FeatureValue=-1 }

Haar feature detection is a multi scale function basis and frequency is generally determined by its scale, not the direction. As many image bases, it forms a laplacian pyramid where its subscale is the subsampled low-resolution version (pre-filtered) of the signal plus a number of basis-projected versions of the signal for the high frequency components of that level. For instance the HWT of an image at a given (frequency) level produces a low freq image (LL, smoothed and subsampled) + a LH, a HL and a HH component corresponding to the 1st, 2nd and 5th pattern describe in the illustration 19. That way the image is transformed to an array of response numbers to these simple patterns and using a correct cascade of haar wavelets appropriate to the size , and orientation of detection this can be used as a tool for generic object detection (Papageorgiou, Oren and Poggio, "A general framework for object detection") [citation needed]

The Viola and Jones detector basically works using this framework to discard portions of the image as "non-faces". To construct an optimal haar cascade the classifier is trained with two image sets , one with faces (for face detection usage) and one with non-faces and an adaptive boosting machine learning algorithm , popularly coined as AdaBoost [citation needed] picks the best features that will drive the face detector.
A sample detection image is the following , using the OpenCV cvHaarDetectObjects implementation and the haarcascade_frontalface_alt.xml cascade. The good response rate of this method was also confirmed by realtime usage on the International Fair of Thessaloniki 2011 where GuarddoG collected over 4500 faces on a course of a week with a very low false detection rate.

Illustration 20: Left : Sample face detected (marked by purple circle) , features detected by the corner detector explained at topic 1.2.1 (marked with yellow dots). Right : a possible HAAR cascade manually created for dramatization of the way HAAR Cascades digitize images and thus serve well for two dimensional face and object detection.

Illustration 21: Random faces out of a 4500+ faces collection gathered during IFT 2011

*after

Mathematical Framework

1.3.0 World Coordinate System

UNDER CONSTRUCTION :P
This is the place where I explain Projective Geometry , Classic geometry , a little about odometry using the motor encoders and the ultrasonic sensors, and the target mapping system , NOT about path planning

*

Mathematical Framework

1.3.1 Epipolar Geometry

Assuming a rectified input of two pinhole cameras with a known alignment , viewing a 3D scene, there are some geometric relations about the projections of 3D points among them.

Both cameras see the world from a different viewpoint , and while the projected image is different there are some geometric constraints that can be leveraged for disparity mapping , a process which will be analyzed later.

GuarddoG's cameras are positioned in parallel so the epipolar plane forms a parallel line from frame to frame. This configuration is used to reduce errors caused by incorrect calibration and reduce the overall complexity of the algorithms that are based on matching parts from one image to the other.
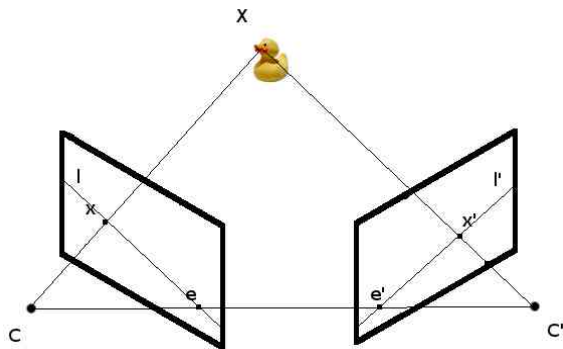

Illustration 23: A non parallel alignment where we can see highlighted the camera centers C and C' , the baseline that goes through both of them , the epipoles e and e' which are the intersections of the image planes with the base line , the projection of the point X at x and x' when connected to the epipoles gives us the epipolar lines l and l'
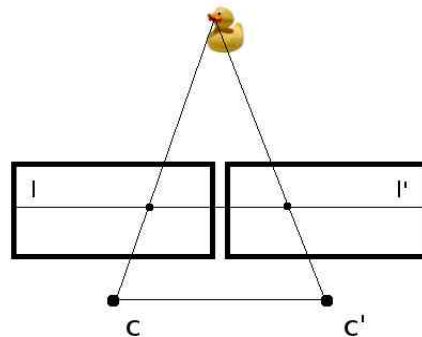

Illustration 22: The parallel alignment used by GuarddoG , all the epipolar lines are parallel. The base line between C and C' does not intersect with the image planes.

*

With the parallel setup the two projection images are essentially being produced by a translation of the camera center parallel to the image plane. This results in the points e and e' being in infinity , and the baseline never touching the image plane (since it is parallel to it)

Since the projection of all the points on the line from C to X and C' to X lay on the l and l' epipolar lines , to find out the projection of the ducks head on the right image we can reduce our search area in the same height coordinates from image to image and that makes disparity mapping practical for computation.

 From a stream of frames (in the axis of time and not space) observed as the robot moves , since we have lots of different types of movements and combinations of rotations and translations , epipolar geometry is once again a useful concept for the calculation of the fundamental matrix between two frames. The reason for this is because it provides the fundamental matrix equation constraints. GuarddoG though uses homographies and not the fundamental matrix for camera pose estimation since the 3d points have a much larger overhead since they have to be extracted through disparity mapping and typically have a higher error rate and lower coverage than the corners that are used for the homographies.
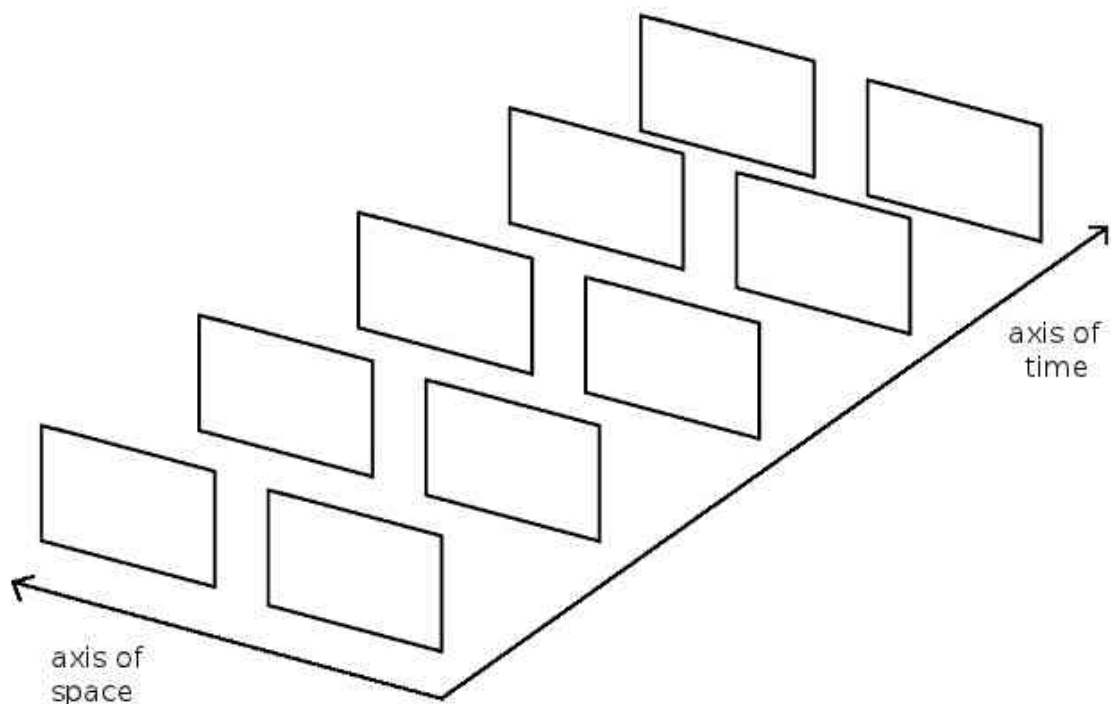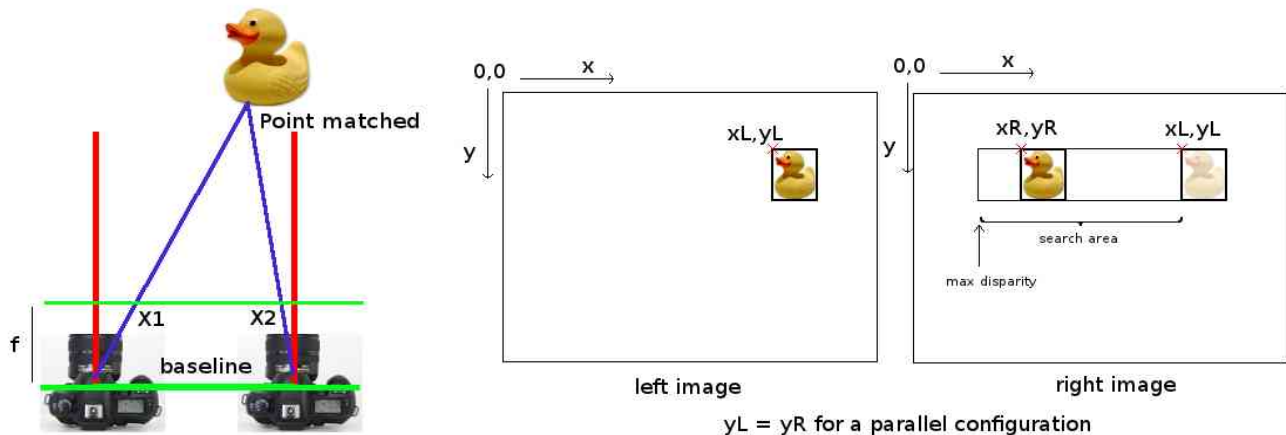

Illustration 24: The stream of incoming images spans both in time and space axis. Epipolar geomtery can help us move in both directions provided that the scene we view as we move remains static.

*

Mathematical Framework

1.3.2 Binocular Disparity Depth Mapping
on a parallel camera setup

Binocular disparity depth mapping is a procedure that uses two image sources as input and produces an output containing depth information about the scene viewed. This is achieved by matching small parts from the left image to the right one and vice versa and calculating the difference of the image region projections.
Due to the complex nature of 3d scenes , occlusions , specular lighting highlights and frequent low texture areas , this is a difficult task especially when computing a dense depth map , since there is a large area to search for every 3D voxel of output.
GuarddoG uses a parallel binocular camera setup on rectified images which simplifies the procedure since , as discussed in the previous topic , epipolar lines are collinear and parallel. This reduces the vagueness of the search domain and and also reduces the total number of operations , which as seen in the overview are in the worst case 24,576,000 comparison operations (using a 10x10 window this means 2,457,600,000 pixel operations) for two 320x240 images.

For performance reasons the resolution of the two images is also 320x240 since due to the target low-end CPU

Typical disparity mapping algorithms use a metric such as SAD , SSD , MSE and others as mentioned in the Template Matching topic of this document. There are many algorithms for disparity mapping which use different approaches and ideas. A great list of related disparity mapping algorithm can be found in the Middleburry benchmark for stereo vision (vision.*middlebury*.edu/stereo/eval) , which is a list of algorithms compared on the same rectified image dataset along with their scores.

The different approaches can be grouped in 3 steps.
1 – Preprocessing the image to make it suitable for the nature of operations on step 2
2 – Performing the comparison operations from one image to the other and storing the results on a depth buffer
3 – Refining the output depth buffer using some smoothness constraints

The first part is typically the fastest part of the procedure , since it does not involve iterations between the

windows on the image. Converting an image to its sobel derivative for example requires 320x240x6 operations and 460,800 operations (much less than the 2,457,600,000 operations worst case for step 2 , this difference has an even larger impact on real cpu time , due to data locality overheads.

In GuarddoG the approach followed is to focus on preparing many representations of the data , and then use raw subtraction on them (with the help of summed area tables) to achieve a dense result with good performance.

$\rightarrow$ Second derivative $\rightarrow$ Summed Area Table Representation

RGB Image $\rightarrow$ Gaussian Blur $\rightarrow$ Sobel Edge $\rightarrow$ Summed Area Table Representation

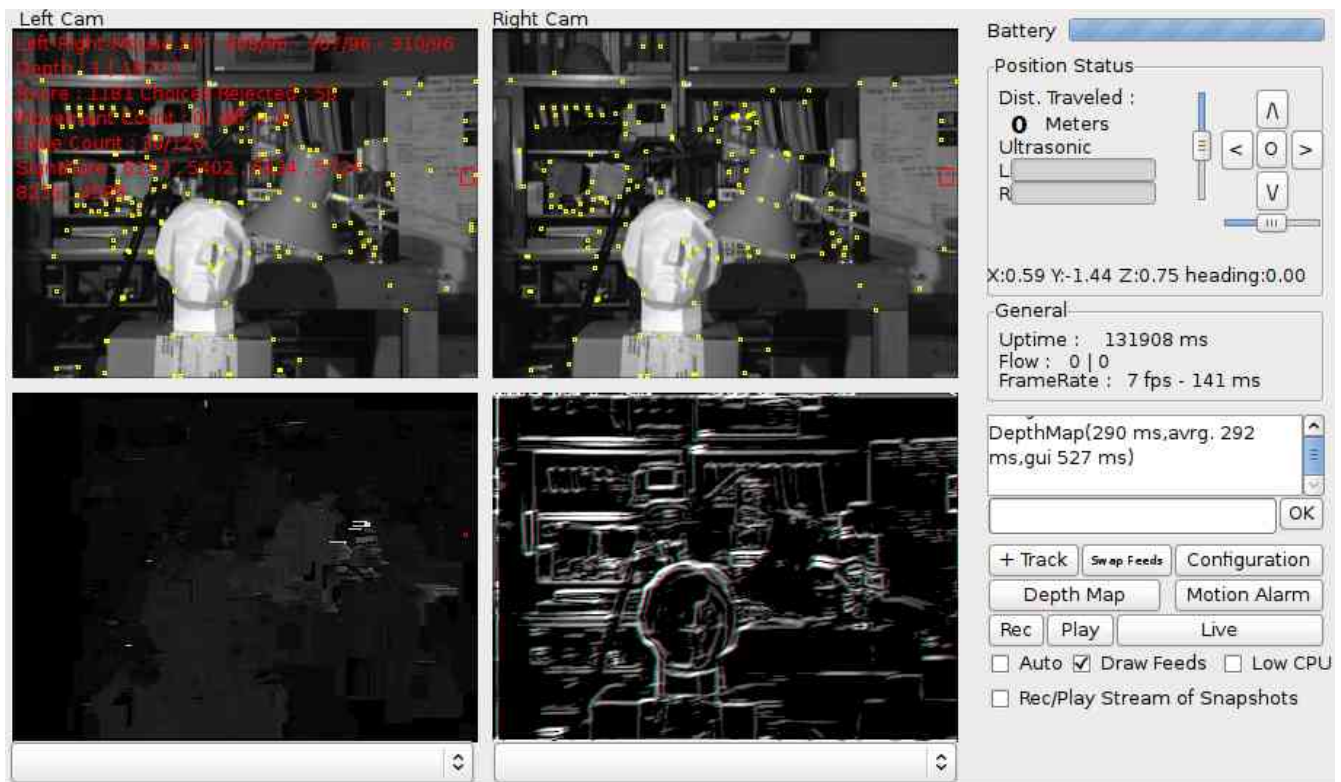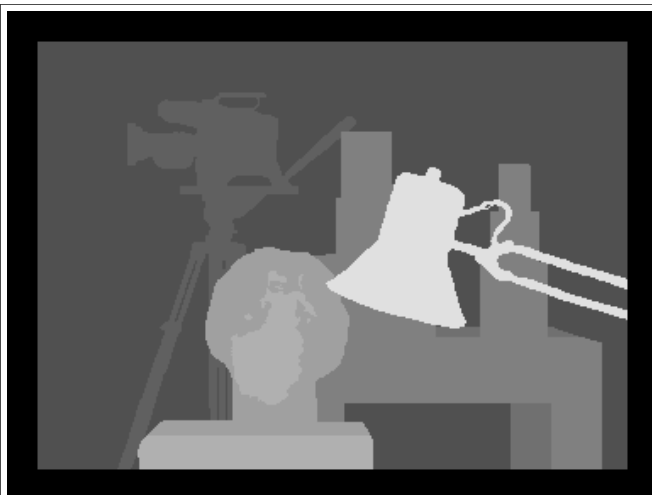RGB (Movement) Difference With last RGB Frame $\rightarrow$ Summed Area Table Representation

Illustration 25: Disparity Mapping on the GUI of GuarddoG

GROUND TRUTH
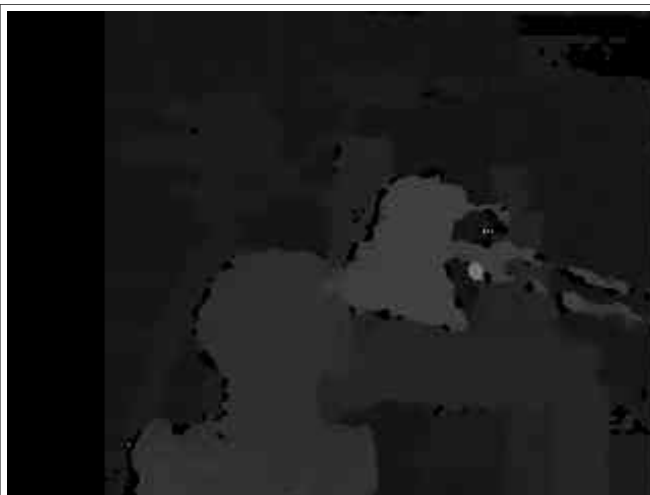
OpenCV BirchfieldTomasi 34 ms
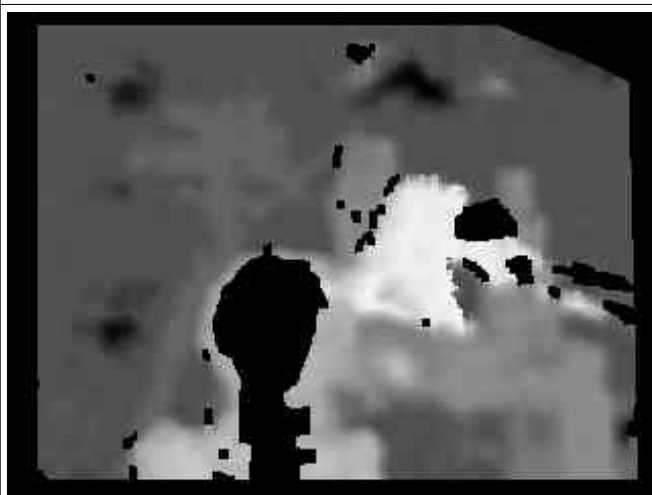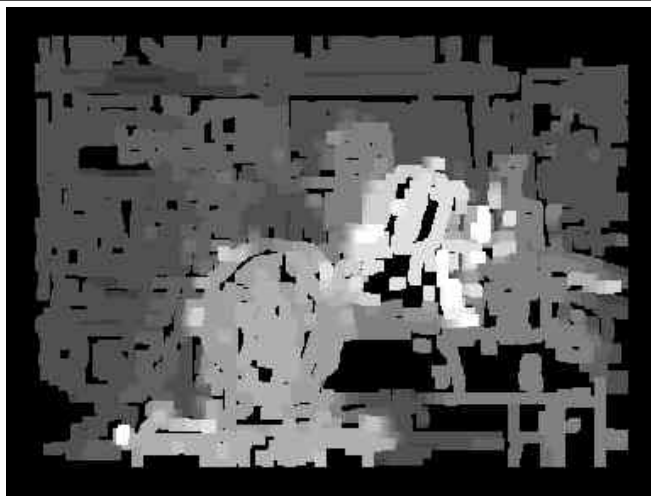
libELAS 52 ms

GuarddoG (quality setting 2) 66 ms
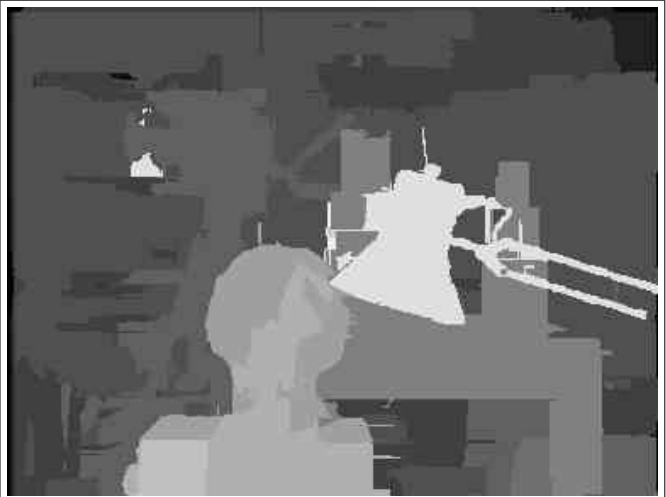
GuarddoG (quality setting 3) 118 ms

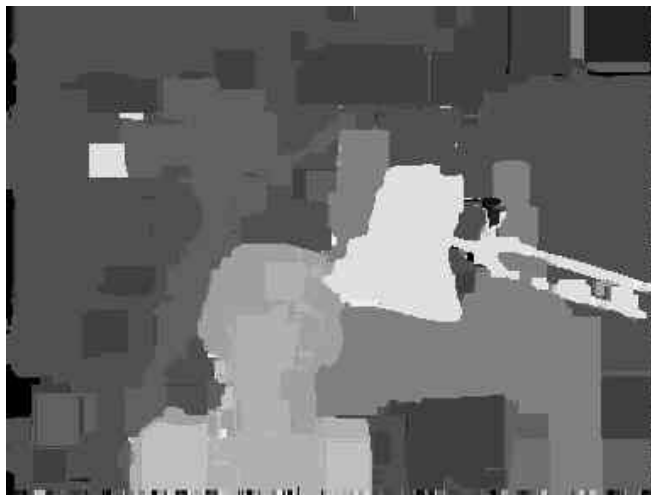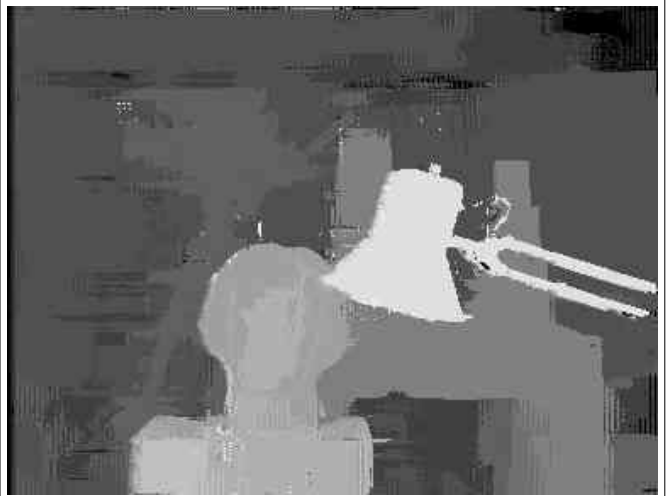**GuarddoG (quality setting 4) 290 ms**

LineSeg 1300+ ms
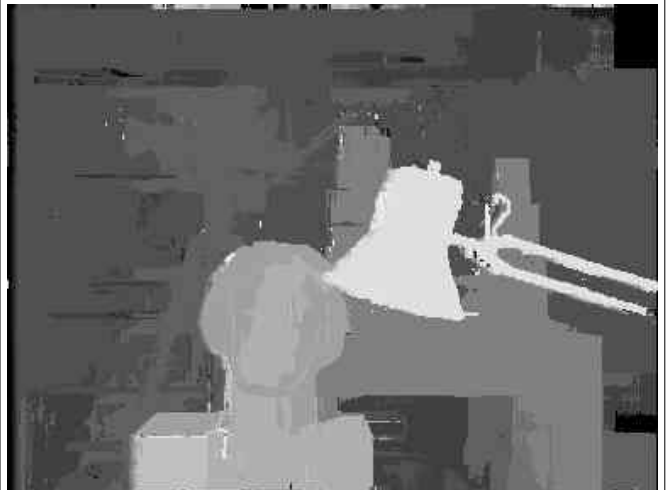
Segmentation Based 2000 ms

Variable Windows 26000 ms

Fast Bilateral 32000ms

Adaptive Weights 1221000 ms

Segment Support 2358000

*

Mathematical Framework

1.1.0 Homography

Given two sets of two dimensional points and the correspondence between them , a problem that arises is calculating the transformation that took place to lead from the first set of points to the other. This is called a homography and being able to find a close approximation of it is a tool that can be used to allow the camera position to be tracked , with purely visual means.

Supposing we have the points : $p_1 (x_1 , y_1 , 1)$, $p_2 (x_2 , y_2 , 1)$ ... $p_n (x_n , y_n , 1)$ which correspond to the points $p'_1 (x'_1 , y'_1 , 1)$, $p'_2 (x'_2 , y'_2 , 1)$ ... $p'_n (x'_n , y'_n , 1)$

We want to find a 3x3 matrix H so that $p'_i = H p_i$ for every i from 1 to n

$$\begin{bmatrix} x'_i \\ y'_i \\ z'_i \end{bmatrix} = H \begin{bmatrix} x_i \\ y_i \\ z_i \end{bmatrix}$$

$$\begin{bmatrix} x'_i \\ y'_i \\ z'_i \end{bmatrix} = \begin{bmatrix} h_{11} & h_{12} & h_{13} \\ h_{21} & h_{22} & h_{23} \\ h_{31} & h_{32} & h_{33} \end{bmatrix} \begin{bmatrix} x_i \\ y_i \\ z_i \end{bmatrix}$$

performing the multiplication

$$\begin{bmatrix} x'_i \\ y'_i \\ z'_i \end{bmatrix} = \begin{bmatrix} h_{11} x_i + h_{12} y_i + h_{13} z_i \\ h_{21} x_i + h_{22} y_i + h_{23} z_i \\ h_{31} x_i + h_{32} y_i + h_{33} z_i \end{bmatrix}$$

for inhomogenous coordinates

$$\begin{bmatrix} x'_i / z'_i \\ y'_i / z'_i \\ 1 \end{bmatrix} = \begin{bmatrix} \dfrac{(h_{11} x_i + h_{12} y_i + h_{13} z_i)}{(h_{31} x_i + h_{32} y_i + h_{33} z_i)} \\ \dfrac{(h_{21} x_i + h_{22} y_i + h_{23} z_i)}{(h_{31} x_i + h_{32} y_i + h_{33} z_i)} \\ 1 \end{bmatrix}$$

Provided we have enough (correct) point correspondences we can form enough equations to find the values of h_{11} , h_{12} ,h_{13} ,h_{21} ,h_{22} ,h_{23} ,h_{31} ,h_{32} ,h_{33} .but due to errors , not only caused by feature detection , but also by the matching procedure even when using subpixel accuracy points that have a high percentage of correct matches the usual case is that the equations cannot be solved as they are incompatible and there is no possible H matrix that can satisfy them.

The solution to the problem is to start picking pairs and then compare their squared differences

$$\sum \left(x'_i - \frac{(h_{11} x_i + h_{12} y_i + h_{13} z_i)}{(h_{31} x_i + h_{32} y_i + h_{33} z_i)} \right)^2 + \left(y'_i - \frac{(h_{21} x_i + h_{22} y_i + h_{23} z_i)}{(h_{31} x_i + h_{32} y_i + h_{33} z_i)} \right)^2$$

Gradually using a point picking algorithm such as RANSAC (the next theory issue examined) that due to its design can be resistant to outlier matches a gradually improving approximation is built.

The OpenCV methods for finding a homography , provided we have first extracted two sets of points and matched them is called `cvFindHomography` and it can use the RANSAC , a least median or a raw method using all of the available points. Due to the importance of pose tracking for the camera of the robot , and despite of the stochastic nature of the algorithm the RANSAC option is chosen by guarddog to compensate for the medium quality of features points and their matches.
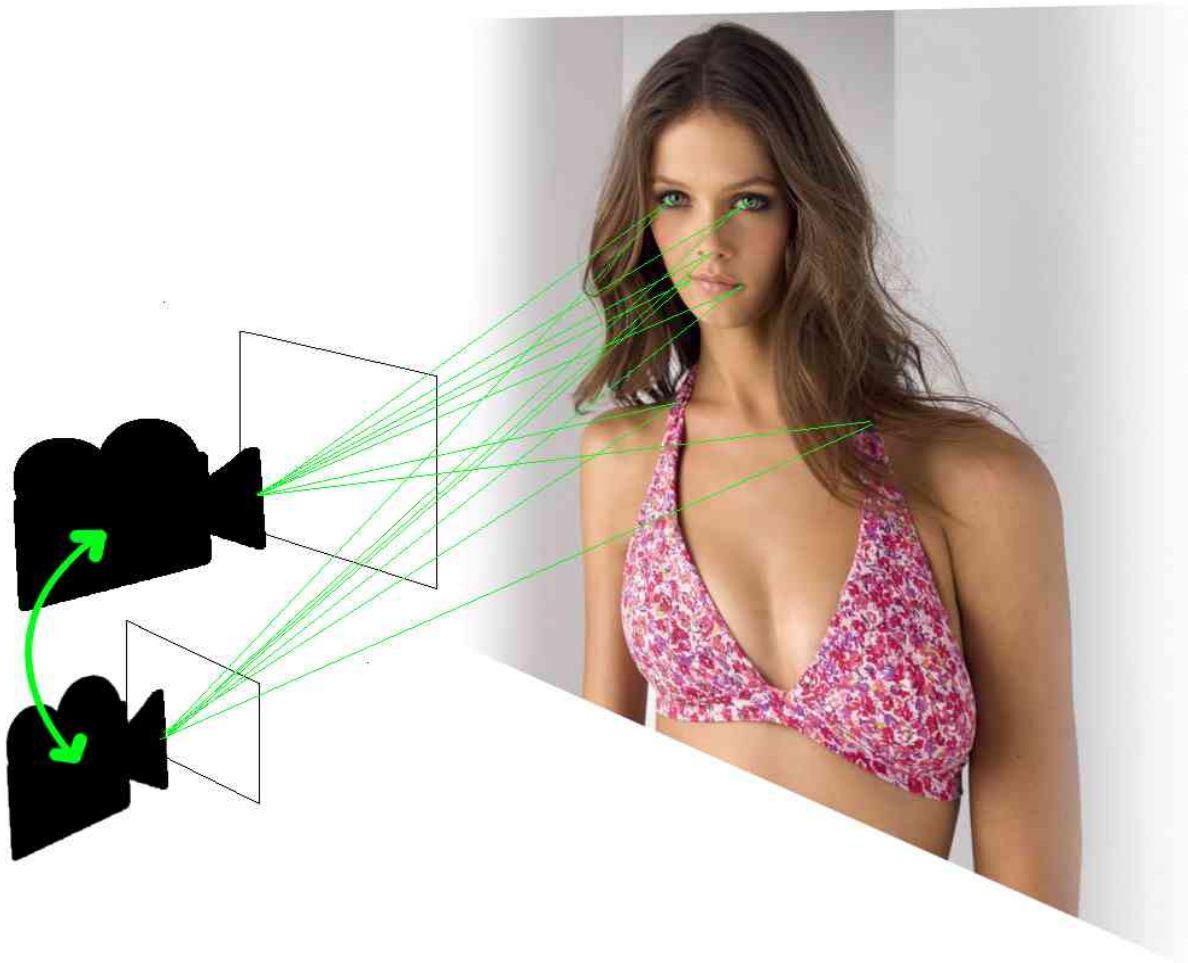

Illustration 26: In a picture and a few words , a homography finds out the transformation that took place between two views of a scene from two matched sets of 2D points

*

Mathematical Framework

1.4.0 RANSAC

RANSAC or RANdom SAmple Consencous is an algorithm that is designed to pick elements from a dataset. It was first published in 1981 [citation needed] and differs from other algorithms that do the same thing because it filters out outliers as part of its process and for a high enough probability of a dataset element being an inlier and a matching configuration it returns an undistorted result. In GuarddoG its main use is refining the homography produced by filtering incorrect feature point correspondances.
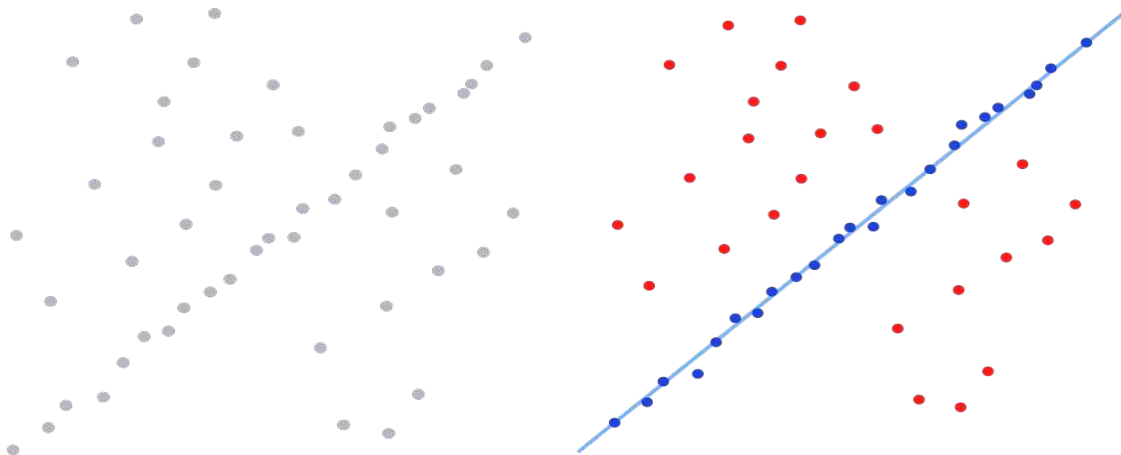
Illustration 27: Left : A collection of points that form a line with a high number of incorrect measurments , Right : RANSAC given criteria to match points along a line can successfully reject outliers and recover the line , Images from Wikipedia , public domain

The algorithm has a model and iteratively picks small subsets of the data and tries to maintain it keeping track of the error rate of a particular subset. Each time a large enough subset fits the model better than all previous ones this is recorded and kept as the new top standard which all feature subsets try to improve. The obvious downside of this algorithm is that it has a very high complexity upper bound for the procedure since it is stochastic (non-deterministic). To improve its performance it can be fitted with a timeout counter that will return after a given time with the best result calculated at the time or it can return the best value when it is satisfactory compared to the maximum acceptable error threshold.

```
RANSAC Algorithm pseudocode :

input:
    data - a set of observations
    model - a model that can be fitted to data
    n - the minimum number of data required to fit the model
    k - the number of iterations performed by the algorithm
    t - a threshold value for determining when a datum fits a model
    d - the number of close data values required to assert that a model fits well
to data
output:
    best_model - model parameters which best fit the data (or nil if no good
model is found)
    best_consensus_set - data points from which this model has been estimated
    best_error - the error of this model relative to the data

iterations := 0
best_model := nil
best_consensus_set := nil
best_error := infinity
while iterations < k
    maybe_inliers := n randomly selected values from data
    maybe_model := model parameters fitted to maybe_inliers
    consensus_set := maybe_inliers

    for every point in data not in maybe_inliers
        if point fits maybe_model with an error smaller than t
            add point to consensus_set

    if the number of elements in consensus_set is > d
        (this implies that we may have found a good model,
        now test how good it is)
        this_model := model parameters fitted to all points in consensus_set
        this_error := a measure of how well this_model fits these points
        if this_error < best_error
            (we have found a model which is better than any of the previous ones,
            keep it until a better one is found)
            best_model := this_model
            best_consensus_set := consensus_set
            best_error := this_error

    increment iterations

return best_model, best_consensus_set, best_error
```

*

Mathematical Framework

1.4.1 Optical Flow

Optical flow is a term describing the process of registering movement on a moving scene. The goal of optical flow algorithms is to robustly track the points on an image as they move and overcome various ambiguities that rise from the incoherent nature of 3d scenes. There are two kinds of optical-flow algorithms , dense and sparse and they differ in the total number of points they are designed to work on. Dense algorithms are generally a lot more computationally expensive and are typically used in monocular setups to perform both tracking and depth estimation. GuarddoG uses stereoscopic disparity mapping to sense depth and thus only needs a sparse optical flow algorithm for matching the corner feature points between frames in order to estimate homographies and track the camera movement .
There are many modeling approaches on building such an algorithm with the most famous being the Lukas Kanade pyramid[citation needed] method , which will be extensively described , the Horn-Schnuck method[citation needed] , work by Black and Anadan [citation needed].
All the algorithms make some basic assumptions about the world they view and regardless of the way the data is processed (using pyramids , velocity fields or other constructs) .

The assumptions for the Lukas Kanade algorithm are the following :

| Assumptions	Details	Weaknesses
Brightness Constancy	Tracked surfaces retain the same color between frames	shadow changes , illumination changes , blinking lights , camera exposure changes , image noise
Temporal Persistence	The rate of movement is sufficiently small between frames.	fast motion , rapid movement , large computation times between frames lead to slower frame rate and thus larger movement between frames
Spatial Coherenece	"Large" enough surfaces move in groups	small particles moving in different directions
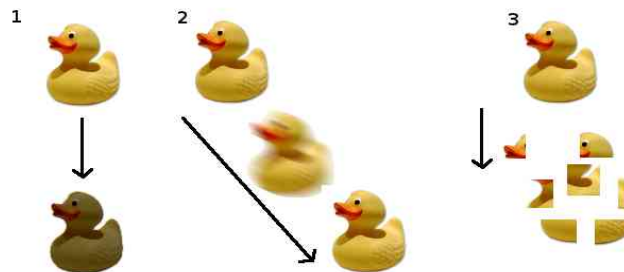
Illustration 28: Some bad instances on the optical flow problem , 1 Brightness constancy violation , 2 fast movement out of the detection window , 3 spatial coherence violated

The assumptions mentioned are translated to mathematical constraints which are checked for being in effect in the neighboring regions of a feature point .

The first one(brightness constancy) is a very straightforward constraint and it basically means that as the time (t) passes , a specific point (f(x)) does not change its light intensity , so the the partial derivative of the change of the pixel value divided by the difference of time between the two frames must be zero.

$$Brightness\ constancy\quad \frac{\partial f(x)}{\partial t}=0$$

The second is the rule of temporal persistence and building on the first rule basically means that for every point I(x , y , t) in a 2D image with coordinates (x, y) and at a specific time (t) has the same intensity response on an area "sufficiently close" in space and time I(x + Δx , y + Δy , t + Δt) , substituting the function I with the partial derivatives it describes and dividing by Δt we get the final equation which has two unknowns , the velocity on the axis x and y , and thus cant be solved , this is were the third constraint comes in.

$$Temporal\ persistence\quad I(x,y,t)=I(x+\Delta x,y+\Delta y,t+\Delta t)$$

$$I(x+\Delta x,y+\Delta y,t+\Delta t)=I(x,y,t)+\frac{\partial I}{\partial x}\Delta x+\frac{\partial I}{\partial t}\Delta y+\frac{\partial I}{\partial t}\Delta t=0$$

$$dividing\ with\ \Delta t\ gives\ us$$

$$(I(x+\Delta x,y+\Delta y,t+\Delta t)-I(x,y,t))\frac{1}{\Delta t}=\frac{\partial I}{\partial x}\frac{\Delta x}{\Delta t}+\frac{\partial I}{\partial t}\frac{\Delta y}{\Delta t}+\frac{\partial I}{\partial t}=0$$

$$\ldots\qquad =\frac{\partial I}{\partial x}V_x+\frac{\partial I}{\partial t}V_y+\frac{\partial I}{\partial t}=0$$

$$\frac{\partial I}{\partial x}V_x+\frac{\partial I}{\partial t}V_y=-\frac{\partial I}{\partial t}$$

Spatial Coherence , provides us with the last tool required. Having a "large enough" image patch moving together allows us to take into consideration all the neighboring points and build more equations to solve for V_x and V_y . The neighborhood can be as large as we want it but a very large window will be easier to violate the coherence constraint , a very small window on the other hand provides less data to work with and suffers from the aperture problem shown in the image.
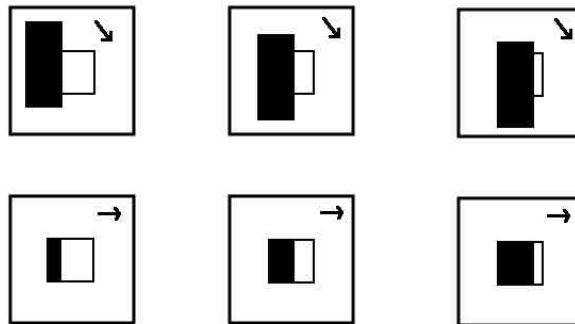

Illustration 29: The aperture problem.
First row : We have a black rectangle moving
diagonally over a small detection window
Second row : Inside the detection window
movement appears to be horizontal

For a 5x5 window e have the following overconstrained system

$$\begin{bmatrix} I_x(P_1) & I_y(P_1) \\ I_x(P_2) & I_y(P_2) \\ ... \\ I_x(P_{24}) & I_y(P_{24}) \\ I_x(P_{25}) & I_y(P_{25}) \end{bmatrix} \begin{bmatrix} V_x \\ V_y \end{bmatrix} = \begin{bmatrix} I_t(P_1) \\ I_t(P_2) \\ ... \\ I_t(P_{24}) \\ I_t(P_{25}) \end{bmatrix}$$

$$A \ v = b$$

This is then solved using a least squares minimization

$$A \ v = b$$
$$A^T A \ v = A^T b$$
$$v = \frac{A^T b}{(A^T A)}$$

$$\begin{bmatrix} V_x \\ V_y \end{bmatrix} = \begin{bmatrix} \sum_i I_x(p_i)^2 & \sum_i I_x(p_i) I_y(p_i) \\ \sum_i I_x(p_i) I_y(p_i) & \sum_i I_y(p_i)^2 \end{bmatrix}^{-1} \begin{bmatrix} -\sum_i I_x(p_i) I_t(p_i) \\ -\sum_i I_y(p_i) I_t(p_i) \end{bmatrix}$$

$A^T A$ is called a structure tensor and this can be solved when $A^T A$ is invertible.
 $A^T A$ is invertible when it has two large eigenvectors and this will happen in areas where texture moves in at least two directions. Thats the reason corners are good tracking features (See corner and feature detection) since they have large two large eigen values.

Though GuarddoG cameras capture frames with a rate of 120 fps on 320x240 and this in theory is a fast enough rate to enforce the temporal persistence , this along with the aperture problem can be mitigated using a gaussian image pyramid , iterating with a variable window.
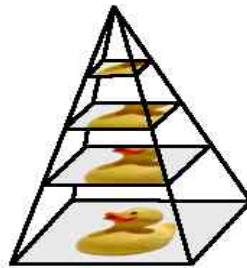

Illustration 30: A gaussian pyramid window

*

Mathematical Framework

1.1.0 Simultaneous localization and mapping

UNDER CONSTRUCTION :P

Markov Localization & Monte Carlo Localization

*

Mathematical Framework

1.1.0 A* Path Finding

Assuming a two dimensional map acquired by the operations above , and a stable track of the position of the robot , there is need for an algorithm to perform path finding , in order for the robot to be able to reach a target position and dynamically change its course when new obstacles are detected. The algorithm used by this project for this kind of functionality is A* , an extension of Dijkstra's graph search algorithm. Successful path finding is very critical because it means less battery drain due to unnecessary movements and better performance as a guard.

A* uses a heuristic that has to never over-estimate the route cost , and such a heuristic is the Manhattan distance that is commonly used by many implementations.
The complexity of the algorithm is $| h(x) - h * (x) | = O(\log h * (x))$ where h is the heuristic used.
The cost of the algorithm for each new node is calculated using $f(n) = g(n) + h(n)$ where g is the cost of the transition to the new node and h the heuristic for the transition to the goal node.
A* is thus admissible since adding g which is an exact estimation of the distance from the source node to the optimistic heuristic since will always make the algorithm seek the solution with the lowest possible cost.
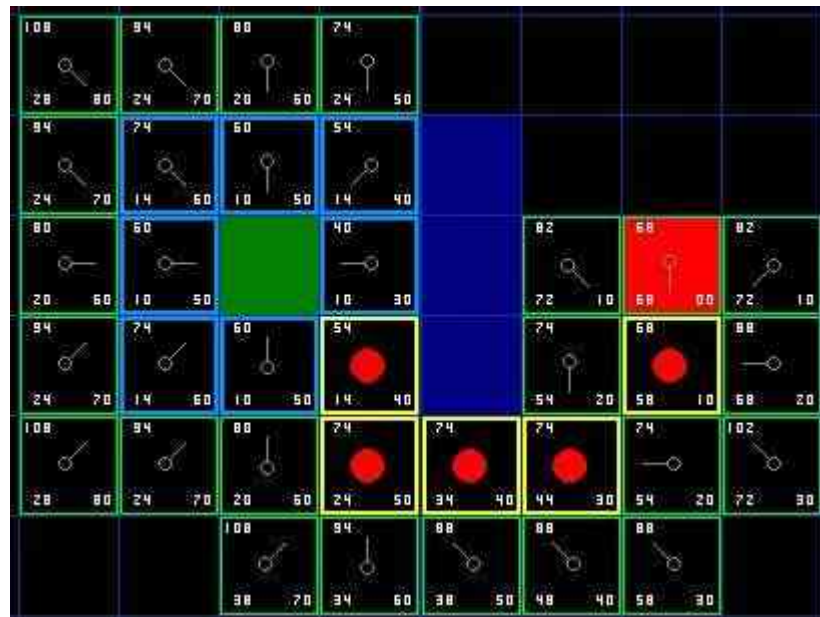
```
A* Algorithm
OPEN SET =  START NODE
CLOSED SET = EMPTY
while the node with the lowest cost in OPEN SET is not the GOAL NODE:
  current = remove lowest rank item from OPEN SET
  add current to CLOSED SET
  for neighbors of current:
    cost = g(current) + movementcost(current, neighbor)
    if neighbor in OPEN and cost less than g(neighbor):
      remove neighbor from OPEN, /*new path is better*/
    if neighbor in CLOSED SET and cost less than g(neighbor):
      remove neighbor from CLOSED SET
    if neighbor not in OPEN SET and neighbor not in CLOSED SET:
        set g(neighbor) to cost
        add neighbor to OPEN SET
        set priority queue rank to g(neighbor) + h(neighbor)
        set neighbor's parent to current

Reconstruct path following parent pointers from goal to start
```

 One of the shortcomings of a raw implementation of an uncustomized A* algorithm is that in the real world diagonal movement is a little further away than than horizontal (pythagorean theorem) . The result is that returned paths can be "non optimal" for a real world moving robot. Added to this problem comes the fact that in physical movement one tends to hold a course turning as little as it is possible. A* can provide an optimal solution that has many turns , but this will take more time for the robot to be traversed. The solution to this problem is keeping the heading of the robot as an information vector on every opened node and adding an extra weight when turns are made , while also adding an extra weight when performing diagonal movement to balance them.

The final element needed is a way to represent uncertainty about the mapped obstacles since there may be errors in the input , not only caused by "mis-detection of obstacles" but also by the the lack of detail of the map since an area of 200 m^2 quantized at a scale of 10 cm^2 per block results in an array sized 2000x1000 that cannot reflect the full complexity of the scene.

Using these modifications , the output becomes better but there is a further improvement that can be achieved by using the largest possible straight paths to connect sub regions of the A* paths. Doing that the turning maneuvers of the robot are reduced to the fewest possible. To achieve that , after a path has been extracted ,instead of reconstructing the path following the parnet pointers we use a second pass algorithm runs which casts a line (using Bresenham's line algorithm) from the last step of the path to all the previous ones until an obstacle is detected. The previous point before the obstacle is then marked as connected to the first one and the algorithm continues until the source node is connected. This improves the operation of the robot . This could also be improved in the future to use odometer based curves instead of point to point turning , something that would also make the movement of GuarddoG seem more life like.
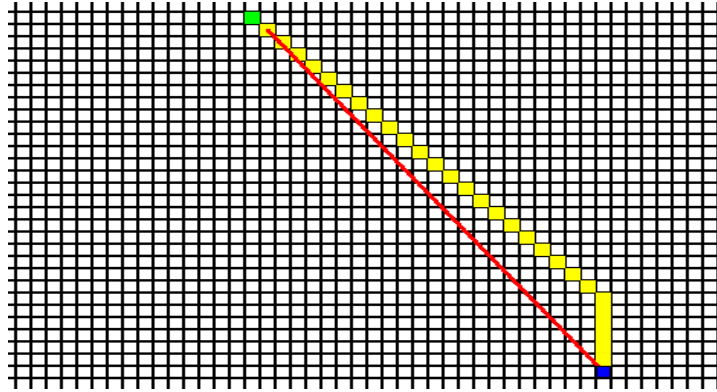
Illustration 31: The problems that may occur using an uncustomized A* Algorithm , and how they are corrected
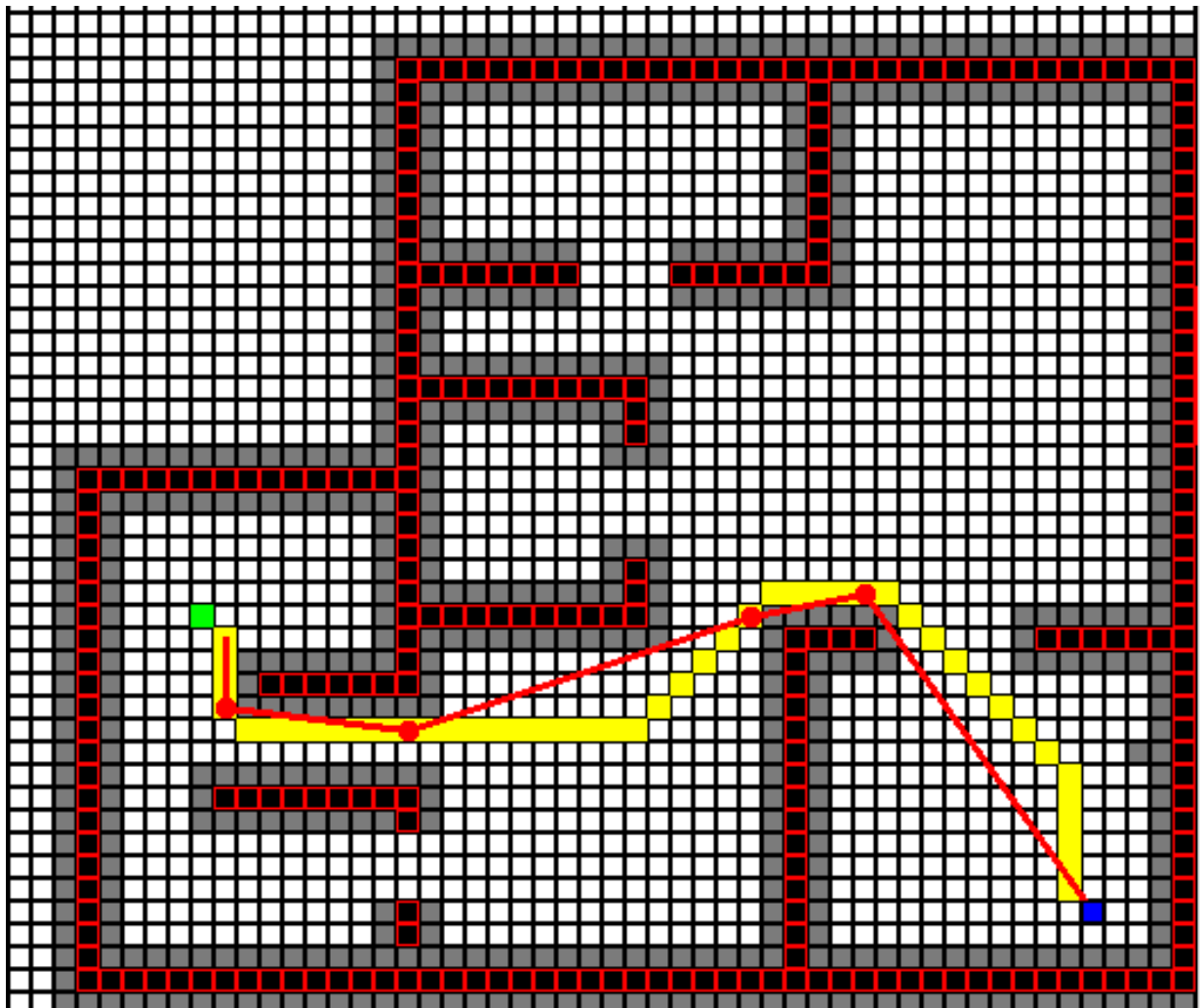
Illustration 32: The green block is the source , the blue the target , red/black blocks are obstacles and gray areas , areas of uncertainty. The yellow path is the one that A* returns and the red line the compressed path for as little turning as possible.

*

Mathematical Framework

1.1.0 First-order logic and a Wumpus like world

Or a Shakey one also taken from Russel & Norvig

UNDER CONSTRUCTION :P

*

Hardware

2.1.0 Camera Sensors

An active-pixel sensor (APS) is an image sensor consisting of an integrated circuit containing an array of pixel sensors, each pixel containing a photodetector and an active amplifier. There are many types of active pixel sensors including the CMOS APS used most commonly in cell phone cameras, web cameras and in some DSLRs. Such an image sensor is produced by a CMOS process (and is hence also known as a CMOS sensor),

and has emerged as an alternative to charge-coupled device (CCD) imager sensors.

The term active pixel sensor was coined by Tsutomu Nakamura who worked on the Charge Modulation Device active pixel sensor at Olympus,[4] and more broadly defined by Eric Fossum in a 1993 paper.[5]

Image sensor elements with in-pixel amplifiers were described by Noble in 1968,[6] by Chamberlain in 1969, [7] and by Weimer et al. in 1969,[8] at a time when passive-pixel sensors – that is, pixel sensors without their own amplifiers – were being investigated as a solid-state alternative to vacuum-tube imaging devices. The MOS passive-pixel sensor used just a simple switch in the pixel to read out the photodiode integrated charge.[9] Pixels were arrayed in a two-dimensional structure, with access enable wire shared by pixels in the same row, and output wire shared by column. At the end of each column was an amplifier. Passive-pixel sensors suffered from many limitations, such as high noise, slow readout, and lack of scalability. The addition of an amplifier to each pixel addressed these problems, and resulted in the creation of the active-pixel sensor. Noble in 1968 and Chamberlain in 1969 created sensor arrays with active MOS readout amplifiers per pixel, in essentially the modern three-transistor configuration. The CCD was invented in 1970 at Bell Labs. Because the MOS process was so variable and MOS transistors had characteristics that changed over time (Vt instability), the CCD's charge-domain operation was more manufacturable and quickly eclipsed MOS passive and active pixel sensors. A low-resolution "mostly digital" N-channel MOSFET imager with intra-pixel amplification, for an optical mouse application, was demonstrated in 1981.[10]

Another type of active pixel sensor is the hybrid infrared focal plane array (IRFPA) designed to operate at cryogenic temperatures in the infrared spectrum. The devices are two chips that are put together like a sandwich: one chip contains detector elements made in InGaAs or HgCdTe, and the other chip is typically made of silicon and is used to readout the photodetectors. The exact date of origin of these devices is classified, but by the mid-1980s they were in widespread use. By the late 1980s and early 1990s, the CMOS process was well established as a well controlled stable process and was the baseline process for almost all logic and microprocessors. There was a resurgence in the use of passive-pixel sensors for low-end imaging applications,[11] and active-pixel sensors for low-resolution high-function applications such as retina simulation[12] and high energy particle detector.[13] However, CCDs continued to have much lower temporal noise and fixed-pattern noise and were the dominant technology for consumer applications such as camcorders as well as for broadcast cameras, where they were displacing video camera tubes.

In 1995, personnel from JPL founded Photobit Corp., who continued to develop and commercialize APS technology for a number of applications, such as web cams, high speed and motion capture cameras, digital radiography, endoscopy (pill) cameras, DSLRs and of course, camera-phones. Many other small image sensor companies also sprang to life shortly thereafter due to the accessibility of the CMOS process and all quickly adopted the active pixel sensor approach.

The cameras used by GuarddoG are based on the OV7720/OV7221 CMOS VGA (640x480) CAMERACHIP Sensor , and are cheap and easy to find as they are the camera system used by the Playstation 3 Gaming Console

Camera Sensor Key Specifications

Array Size	640 x 480
Power Supply Digital Core Voltage	1.8VDC + 10%
Power Supply Analog Voltage	3.0V to 3.3V
Power Supply I/O Voltage	1.7V to 3.3V
Power Requirements - Active	120 mW typical (60 fps VGA, YUV)
Power Requirements - Standby	< 20 µA
Temperature Range	-20°C to +70°C
Output Format (8-bit)	• YUV/YCbCr 4:2:2 • RGB565/555/444 • GRB 4:2:2 • Raw RGB Data
Lens Size	1/4"

Max Image Transfer Rate	60 fps for VGA
Scan Mode	Progressive
Electronic Exposure	Up to 510:1 (for selected fps)
Pixel Size	6.0 μm x 6.0 μm
Fixed Pattern Noise	< 0.03% of VPEAK-TO-PEAK
Image Area	3984 μm x 2952 μm
Package Dimensions	5345 μm x 5265 μm

*

Hardware

2.1.0 Camera Synchronization

Stereo vision on a mobile robot is a non-trivial problem that traditionally requires expensive hardware-synchronized cameras. Because standard stereo reconstruction assumes that the images from the left and right cameras are captured from a common scene , any motion that occurs between the left and right cameras

capturing frames is equivalent to a change in the stereo camera`s baseline. This change in baseline invalidates the system`s extrinsic calibration , causing the quality of the rectification to decrease and the distances to be distorted by the robot`s velocity.

Hardware synchronization , the process of forcing two or more cameras to share a common hardware clock , has been traditionally limited to the professional stereo vision systems such as Point Grey`s Bumblebee product line . Thankfully , the inexpensive Playstation Eye camera is built on the same high-end OmniVision OV7720 chipset that is comparable to those found in many machine vision cameras. These cameras can be hardware-synchronized using the exposed frame clock input (FSIN) and output (VSYNC) pins . By shorting one camera`s VSYNC pin to the others cameras FSIN pins the cameras are forced to share a common clock . To reduce the risk of a difference in ground potentials damaging the OV7720 delicate circuitry , each camera was also modified to share a common ground .

This hardware synchronization guarantees that all three cameras capture images simultaneously , but does not guarantee that the frames will travel retaining their synchronization on the USB .

Each camera has its own hardware clock and that means that in addition to the small distortion in space (due to optics) we have a small distortion in the fourth dimension , the axis of time. To tackle this problem guarddog uses cameras that have a very fast refresh rate of 120fps @ 320x240 pixels with a rewired shutter (FSIN , VSYNC pins) in order for synchronization on the hardware side of the camera snapshots. A secondary problem is that there is non uniform latency over the USB cable and the USB host controller . This is problem is combated using direct frame grabbing via V4L2 and zero-copy passing by pointer to the beginning of the image pipelining and static linkage of the libraries consisting of the project to reduce delays and overheads.

*

Hardware

2.1.0 USB Host

A USB system has an asymmetric design, consisting of a host, a multitude of downstream USB ports, and multiple peripheral devices connected in a tiered-star topology. Additional USB hubs may be included in the tiers, allowing branching into a tree structure with up to five tier levels. A USB host may have multiple host controllers and each host controller may provide one or more USB ports. Up to 127 devices, including hub

devices if present, may be connected to a single host controller.

USB devices are linked in series through hubs. There always exists one hub known as the root hub, which is built into the host controller.

A physical USB device may consist of several logical sub-devices that are referred to as device functions. A single device may provide several functions, for example, a webcam (video device function) with a built-in microphone (audio device function). Such a device is called a compound device in which each logical device is assigned a distinctive address by the host and all logical devices are connected to a built-in hub to which the physical USB wire is connected. A host assigns one and only one device address to a function.

Diagram: inside a device are several endpoints, each of which is connected by a logical pipes to a host controller. Data in each pipe flows in one direction, although there are a mixture going to and from the host controller. USB endpoints actually reside on the connected device: the channels to the host are referred to as pipes

USB device communication is based on pipes (logical channels). A pipe is a connection from the host controller to a logical entity, found on a device, and named an endpoint. Because pipes correspond 1-to-1 to endpoints, the terms are sometimes used interchangeably. A USB device can have up to 32 endpoints: 16 into the host controller and 16 out of the host controller. The USB standard reserves one endpoint of each type, leaving a theoretical maximum of 30 for normal use. USB devices seldom have this many endpoints.

There are two types of pipes: stream and message pipes depending on the type of data transfer.

　　isochronous transfers: at some guaranteed data rate (often, but not necessarily, as fast as possible) but with possible data loss (e.g., realtime audio or video).

　　interrupt transfers: devices that need guaranteed quick responses (bounded latency) (e.g., pointing devices and keyboards).

　　bulk transfers: large sporadic transfers using all remaining available bandwidth, but with no guarantees on bandwidth or latency (e.g., file transfers).

　　control transfers: typically used for short, simple commands to the device, and a status response, used, for example, by the bus control pipe number 0.

*

Hardware

2.1.0 Embedded System

V4L2 mmap()

Name

v4l2-mmap -- Map device memory into application address space

Synopsis

#include <unistd.h>
#include <sys/mman.h>

void *mmap(void *start, size_t length, int prot, int flags, int fd, off_t offset);

Arguments

start

   Map the buffer to this address in the application's address space. When the MAP_FIXED flag is specified, start must be a multiple of the pagesize and mmap will fail when the specified address cannot be used. Use of this option is discouraged; applications should just specify a NULL pointer here.

uATX (6.75 inches by 6.75 inches [171.45 millimeters by 171.45 millimeters]) (ITX compatible)
Integrated Intel® Celeron® 220 processor (1.2 Ghz) with a 533 MHz system bus
One 240-pin DDR2 SDRAM Dual Inline Memory Module (DIMM) sockets
Support for DDR2 677/533/400 MHz DIMMs
Support for up to 1 GB of system memory
SiS* SiS662 Northbridge
SiS* SiS964L Southbridge
ADI* AD1888 audio codec
Integrated SiS Mirage* 1 graphic engine
Winbond* W83627DHG-B based Legacy I/O controller for hardware management, serial, parallel, and PS/2* ports

Booting from a USB STICK

Hardware
The Energy − Weight − Heat − Cost Problem

Hardware
GuarddoG Part List / Specifications

Embedded Electronics
1x Arduino = 25 euro (Uno)
3x Infrared Led = 3 euro
1x RD-01 (or RD-02 Devantech motors) = 130 euro
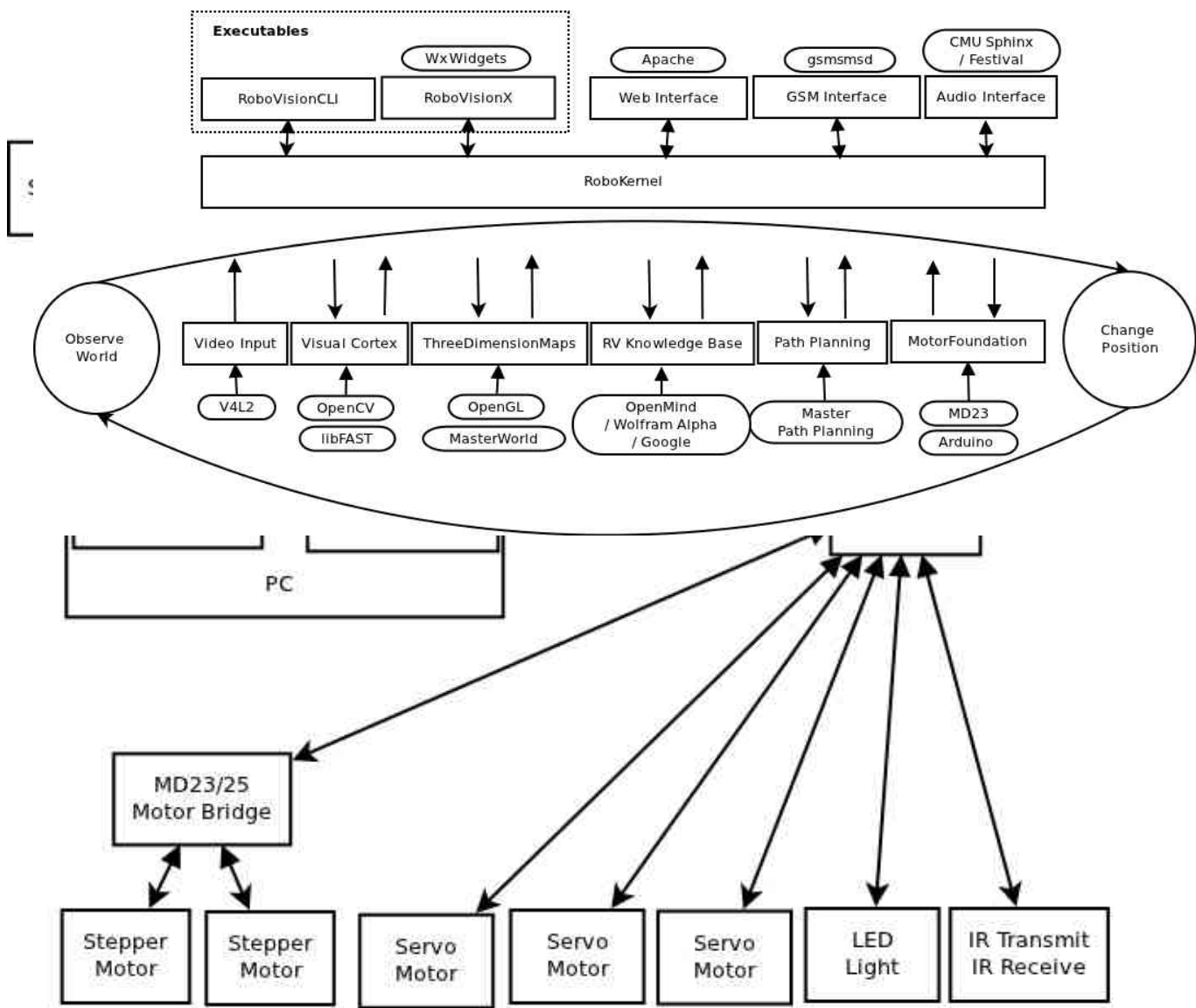2x Buttons (power -on) = 2 euro

2x Switches (power supply) = 2 euro
2x LED HeadLights = 10 euro
2x Ultrasonic Devantech SRF-05 with mounting = 40 euro
1x Dual Axis Accelerometer (memsic 2125) = 30 euro
Total : 252 euro

Computer Hardware

1x Fan = 5 euro
1x Mini-Itx Motherboard = 65-75 euro (Currently on guarddog Intel D201GLY2)
1x PicoPSU 90W = 45 euro
1x AC-DC 12 V Converter = 30 euro
2x Webcams (On guarddog MS VX-6000) = 92 euro , LOGITECH C510 HD , PS3 Eyes
1x WIFI PCI card (WG311T) = 30 euro
1x USB Flash Drive 8GB + = 20 euro
1x 512-2048MB RAM DIMM (on guarddog 512MB DDR2) = 30 euro
Total : 327 euro

Software Stack
Pipeline Outline

BIOS → MBR → GRUB → Kernel /sbin/init → Runlevel Initialization →

GuarddoG Service Start

RAM Runtime
Filesystem Preperation and
File Copying

gsmsmsd

Apache
Web Server

RoboVision CLI
or
RoboVisionX

SMS Interface
Thread

WebInterface
Thread

RoboKernel
Thread

MD23
Thread

Motor HAL
Thread

VideoInput
Thread

Arduino
Thread

ScriptRunner
Thread

Activity
Thread

VisualCortex
Thread

Software Stack
Performance Hypervisor

Software Stack
Implementation Framework

Software Stack
Statistics

The System in Practice
Installation

The System in Practice
Data Sets and Test Results

The System in Practice
Commercial Value

The System in Practice
Weaknesses

Future Work
Network Connectivity
NLP – AI Knowledge Base
Speech Recognition
Commercial Robots
CUDA / VLSI acceleration

Acknowledgements

*

Bibliography / References

[1]
[2]
[3]A Flexible New Technique for Camera Calibration (1998) by Zhengyou Zhang , Zhengyou Zhang
[4]Edward Rosten , Fusing points and lines for high performance tracking , (**YEAR HERE**) Machine learning for high-speed corner detection.
[5] Herbert Bay, Andreas Ess, Tinne Tuytelaars, Luc Van Gool, (**YEAR HERE**) SURF: Speeded Up Robust Features
[6]Jianbo Shi , Carlo Tomasi , (YEAR HERE) Good Features to Track
[7]Yoav Freund, Robert E. Schapire. "A Decision-Theoretic Generalization of on-Line Learning and an Application to Boosting", 1995